

Multi-component (high entropy) alloys as a basis for new generation of high- temperature materials

S.A.Firstov
IPMS NASU

sfirstov@ukr.net

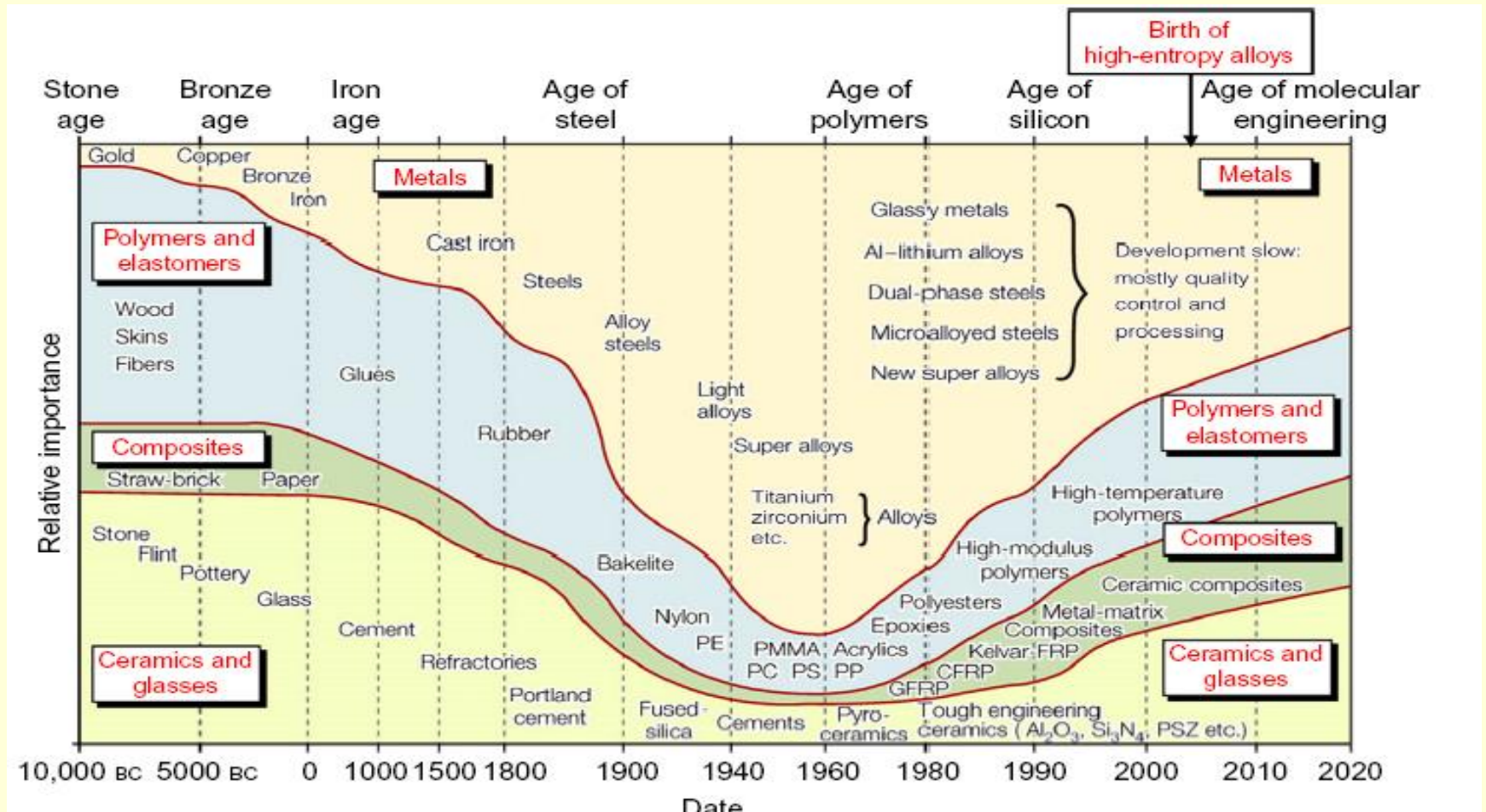
**"Materials resistant to extreme conditions for future energy systems"
12-14 June 2017, Kyiv - Ukraine**

Outlook

- ***Introduction***
- ***Structure peculiarities***
- ***Non-obvious solid solutions hardening***
- ***High-temperature applications***
- ***New composites***
- ***Conclusions***

Historical evolution of engineering materials

(adopted from Ashby (2011))

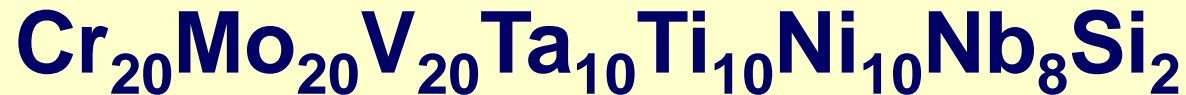


- **Inoue A.**, Stabilization of metallic supercooled liquid and bulk amorphous alloys. *Acta Mater.* **2000**, **48**, 279-306. 2.
- **Ranganathan S.** Alloyed pleasures: Multimetallic cocktails // *Current Science.* – **2003.** – **85**, No. 7. –. P. 1404-1406.
- **Yeh J.W., Chen S.K., Lin S.G. et al.** Nanostructured high entropy alloys with multiple principal elements: Novel alloy design concepts and outcomes // *Adv Eng Mater*, **2004**, **6**: 299–303.
- **Huang K. H.** A study on the multi-component alloy system containing equal-mole elements. *Master Degree Thesis National Tsing Hua University in Taiwan*, **1995 !**

High entropy alloys

“For the high-entropy alloys, solid solution can be formed by alloying, and its mechanical properties can be comparable to most of the bulk metallic glasses”

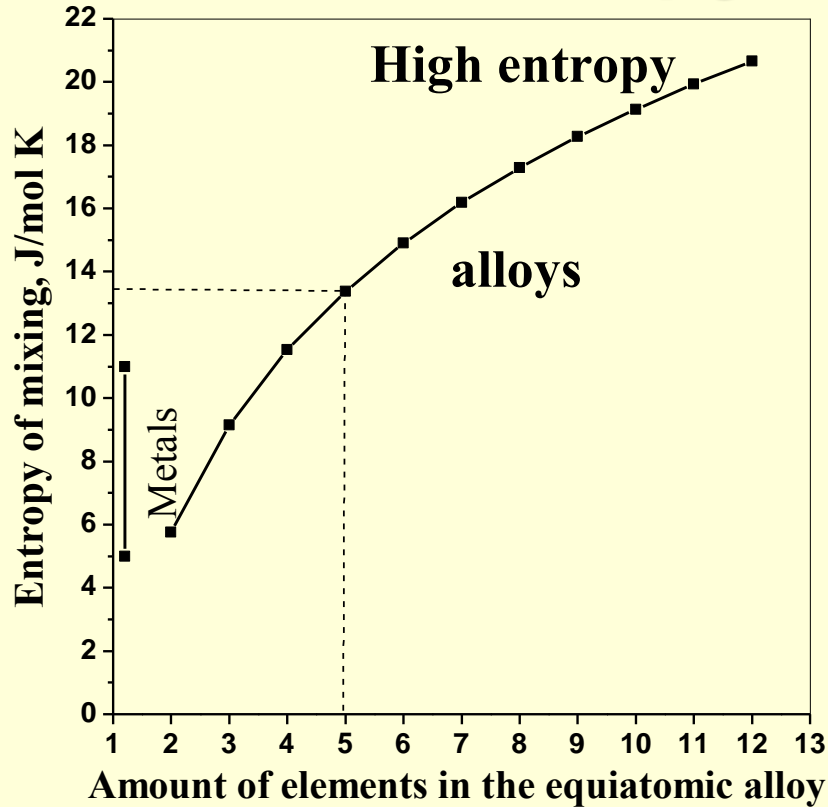
(Yong Zhang, YunJun Zhou, XiDong Hui, MeiLing Wang and GuoLiang Chen, 2008)



There is no “host element”;

It is not possible to say: Alloy based upon...

Entropy of mixing



Boltzman:

$$\Delta S_{\text{mix}} = -R \sum_{i=1}^n c_i \ln c_i;$$

$$R=8,314 \text{ J} \cdot \text{mol}^{-1} \text{ K}^{-1}$$

1995 – Jien-Wei Yeh

HEA – multicomponent alloys

more than 5 elements –

$$5 \geq c_i \leq 35 \text{ at. \%}$$

$$\Delta S_{\text{mix}} > 13.38 \text{ J mol}^{-1} \text{ K}^{-1}$$

Consequences of high entropy:

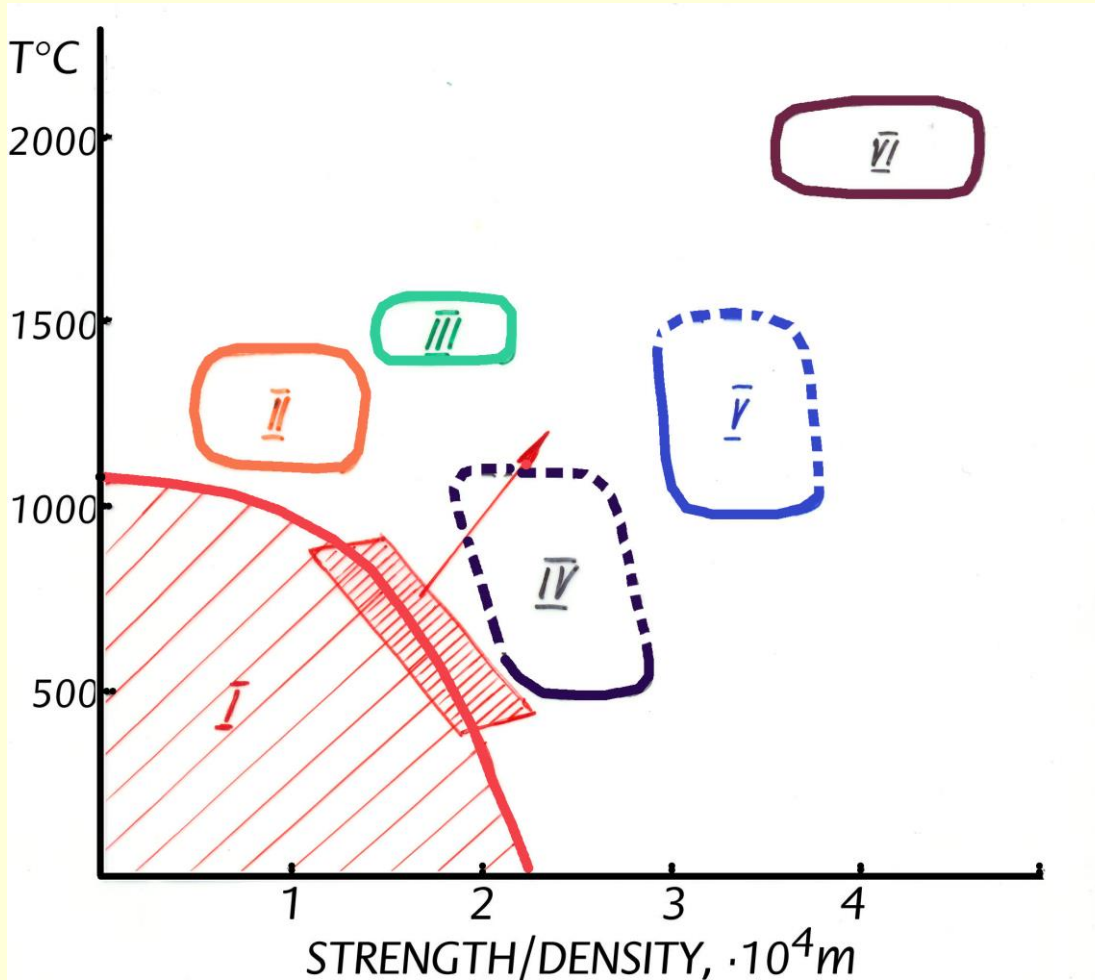
High thermal stability due to $\Delta G = \Delta H - T\Delta S$, including lower tendency towards segregation and ordering;

The total number of the forming phases is well below the maximum equilibrium number allowed by the Gibbs phase rule

Severe lattice distortion takes place, which lead to the significant solution hardening

Material's high entropy consequences

- **Thermal stability!**
- **Quantity of the forming phases in reality is surprisingly small**



I - Conventional materials, Ti and superalloys

II – Metal matrix composites

III – Ceramics

IV – Intermetallic composites and intermetallic

V – Ceramic composites

VI – Carbon / carbon composites

Possible types of high-entropy alloys

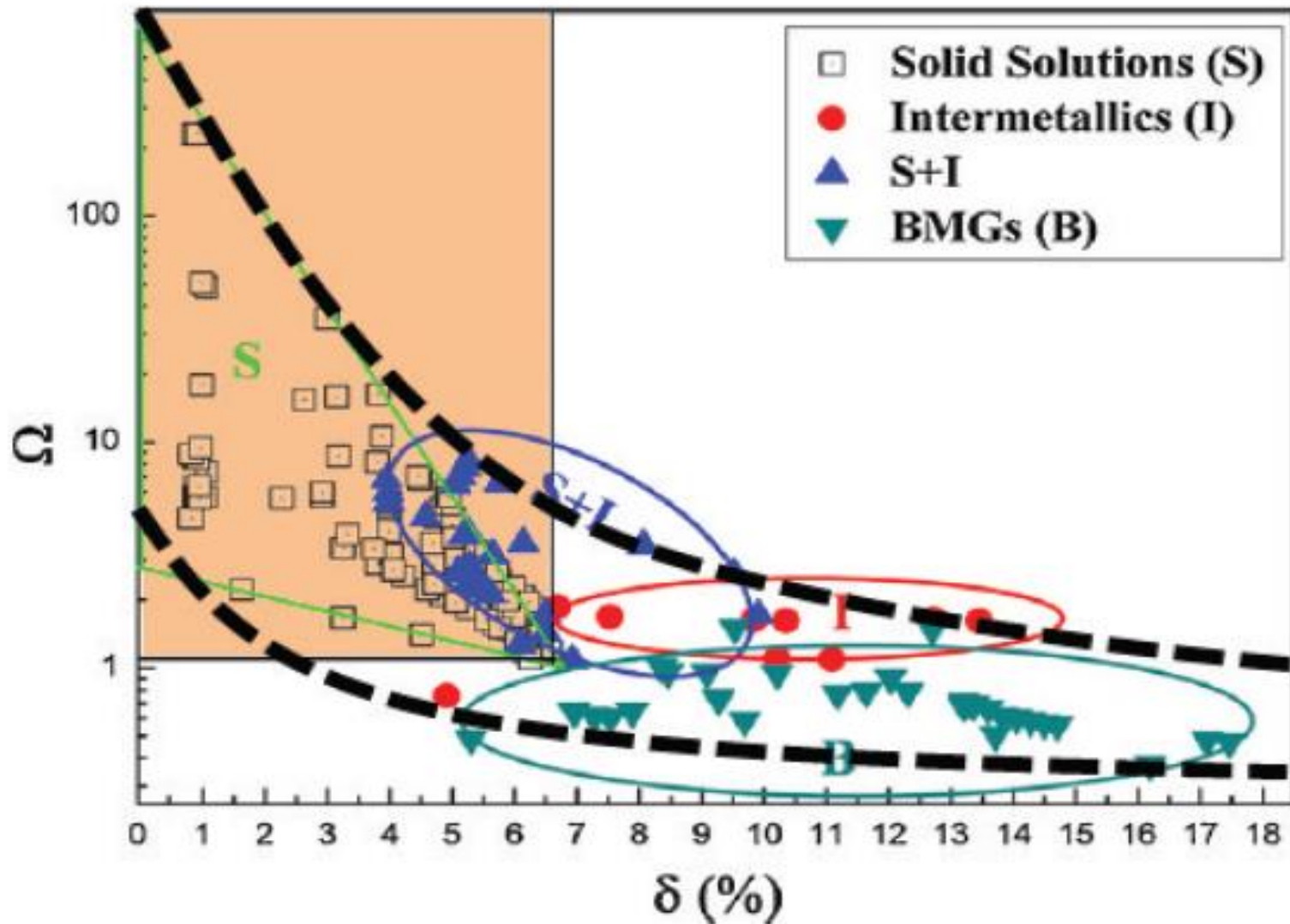
- 1 – Amorphous – crystalline phase is absent.**
- 2 – Single-phase – BCC, FCC - solid solution.**
- 3 – Two-phase – two BCC-solid solutions with different lattice parameters. BCC+FCC or BCC+hexagonal lattice.**
- 4 – Three-phase – BCC-BCC-FCC; BCC-HCP-FCC.**
- 5 – Intermetallic phases – Laves phase (c-14, c-15), σ -phase type of CrF, hexagonal lattice - type of Fe_3Mo_2**

Important factors

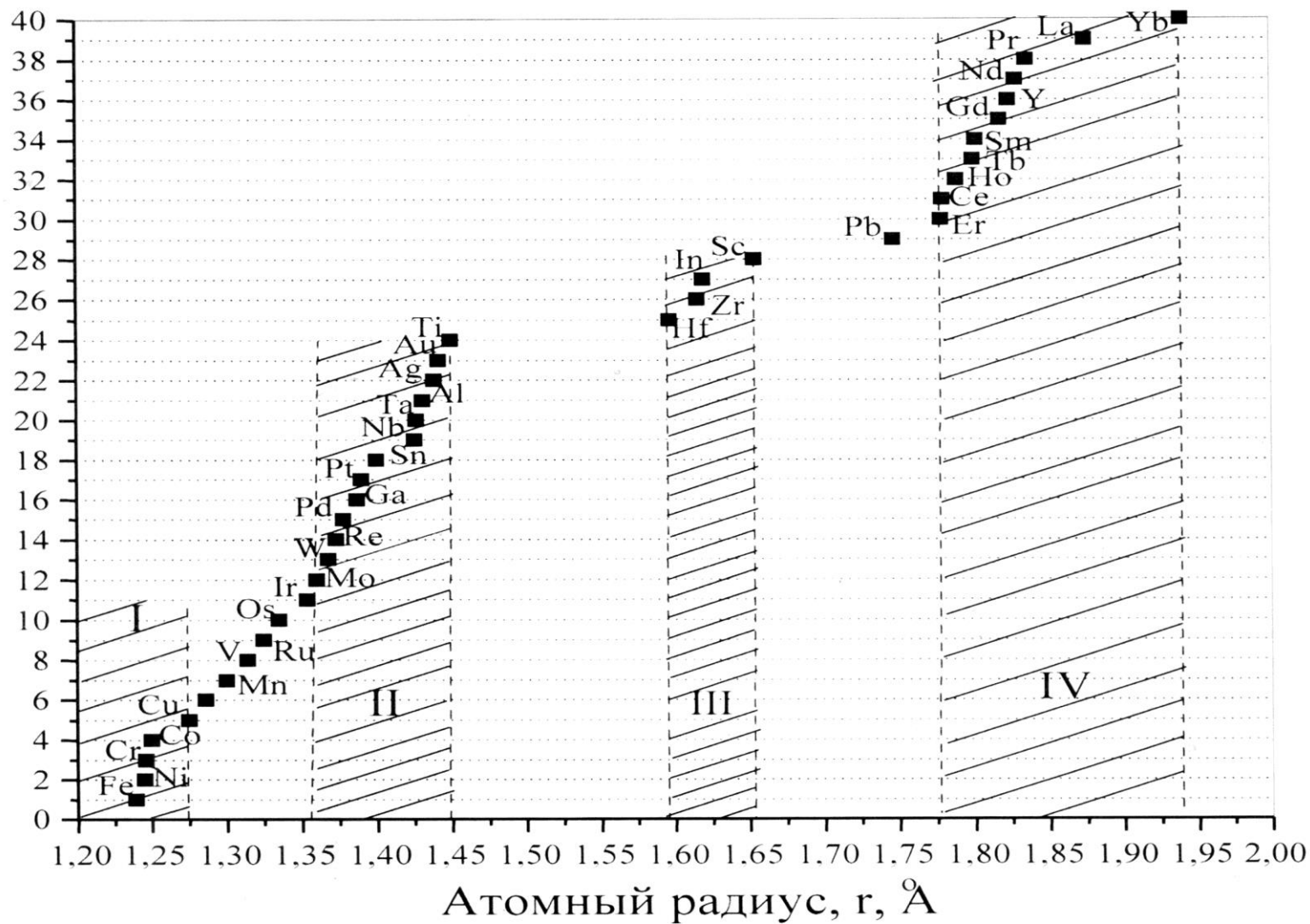
- **Atom sizes difference**
- **Electron-per-atom ratio**
- **Mixing enthalpy**
- **Entropy**

$$\Omega = T_m \Delta S_{\text{mix}} / |\Delta H_{\text{mix}}|$$

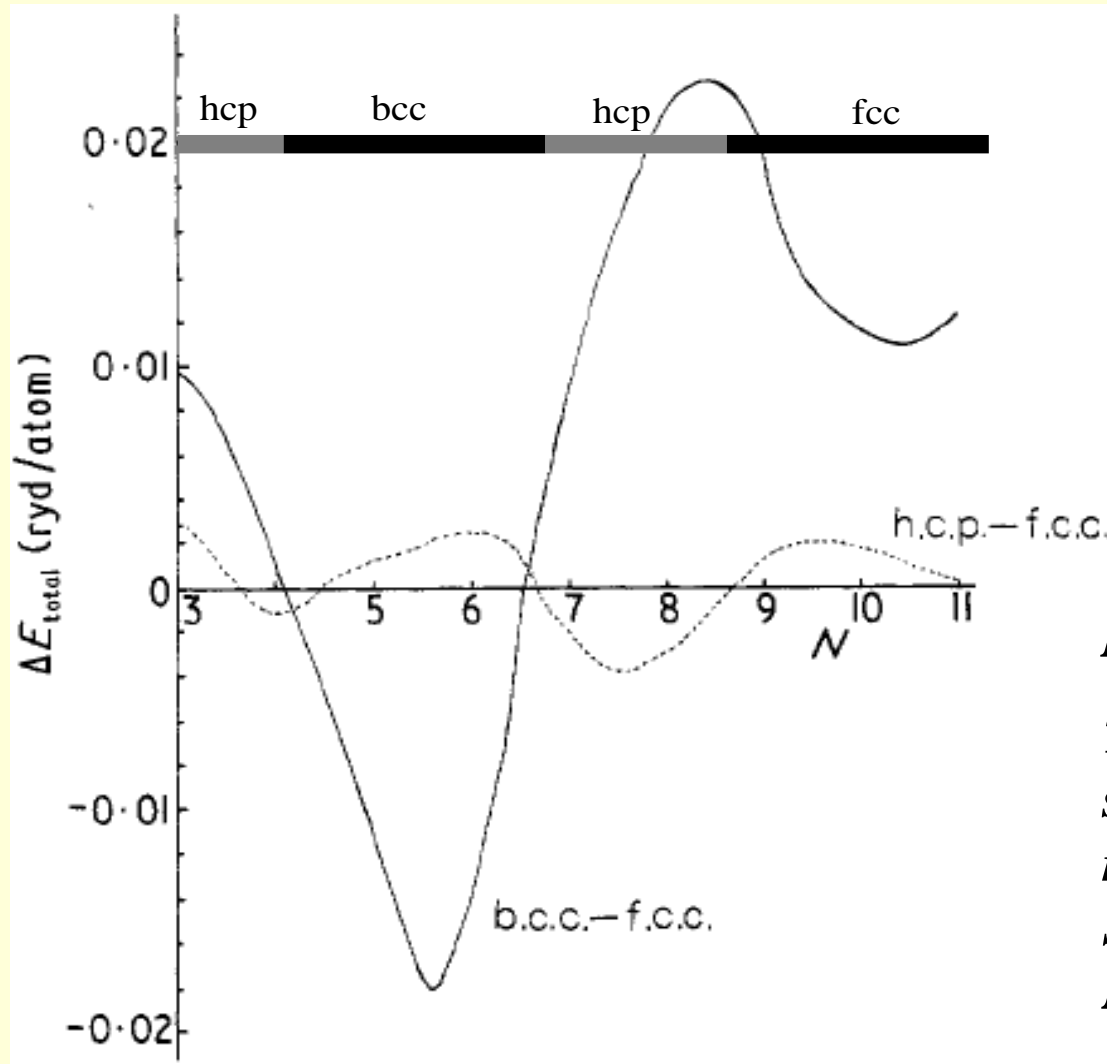
$$G_{\text{mix}} = \Delta H_{\text{mix}} - T \Delta S_{\text{mix}}$$



Atomic radii of metals



Stability of crystal structures by Pettifor (1970)



D.G. Pettifor

Theory of the crystal structure of transition metals J. Phys. C: Solid State Phys., 1970, vol. 3, P. 367-377.

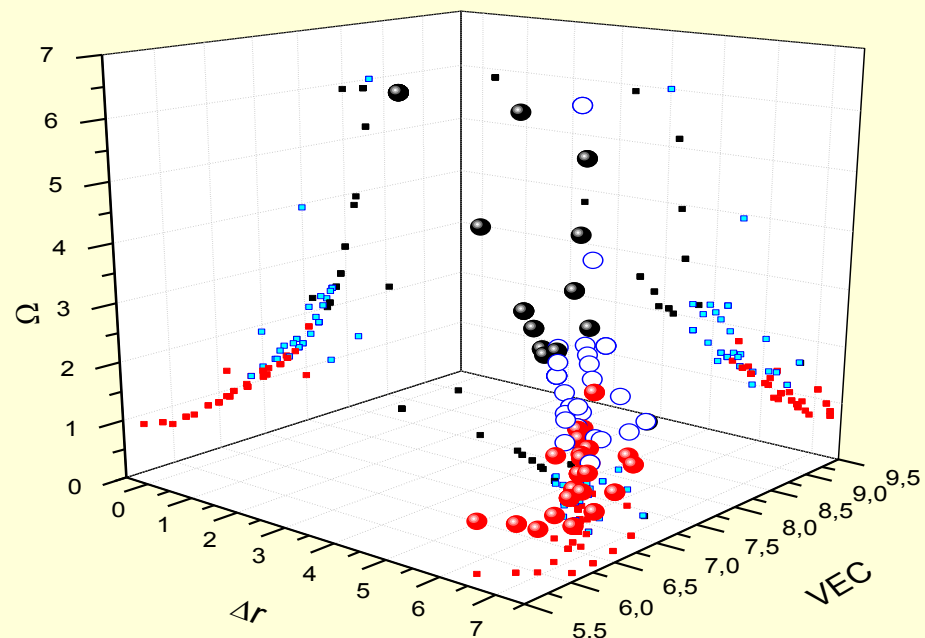
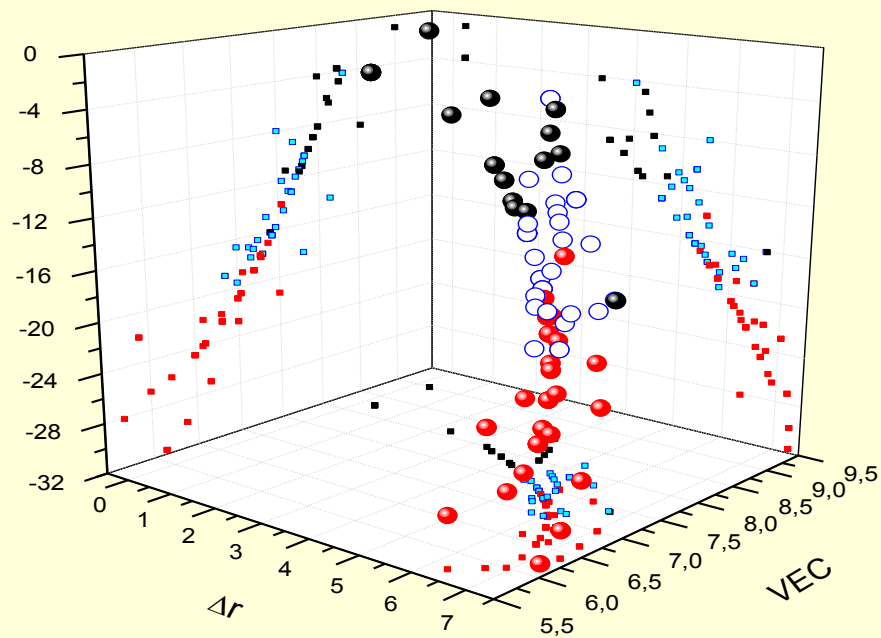
Solid solutions: lattice type vs. e/a

<i>Composition</i>	<i>e/a</i>	<i>lattice</i>
TiZrHfScY	3.6	HCP
TiZrHfScV	4.0	HCP + BCC
Ti ₂₅ Zr ₂₅ Hf ₂₅ Nb _{12,5} Ta _{12,5}	4.25	BCC
TiZrHfVTa	4.4	BCC
TiZrHfVTaW	4.7	BCC + BCC
TiZrHfVNbMo	4.7	BCC
AlTiVCrNbMo	4.8	BCC
VTaCrMoW	5.6	BCC
ReMoWVN	5.8	BCC
ReMoWNbTa	5.8	BCC
FeCoNiCrAl	7.2	BCC

Solid solutions: lattice type vs. e/a

<i>Composition</i>	<i>e/a</i>	<i>lattice</i>
CoNiCuAlCrVMn	7.3	FCC +BCC
FeCoNiCu _{0,5} CrAl	7,54	FCC + BCC
AlCrMnFeCoNiCu	7.7	FCC + BCC
AlCrFe _{0,5} CoNiCu	7.8	FCC + BCC
AlCrFeCoNiCu	7.83	FCC + BCC
AlCrFe ₂ CoNiCu	7.85	FCC + BCC
AlCrFe ₃ CoNiCu	7.875	FCC +BCC
CrWFeCoNiCu	8.3	FCC +BCC
CrMnFeCoNiCu	8.5	FCC
FeCoNiCuCr	8.8	FCC
CrMnFeCoNiCu ₃	9.1	FCC

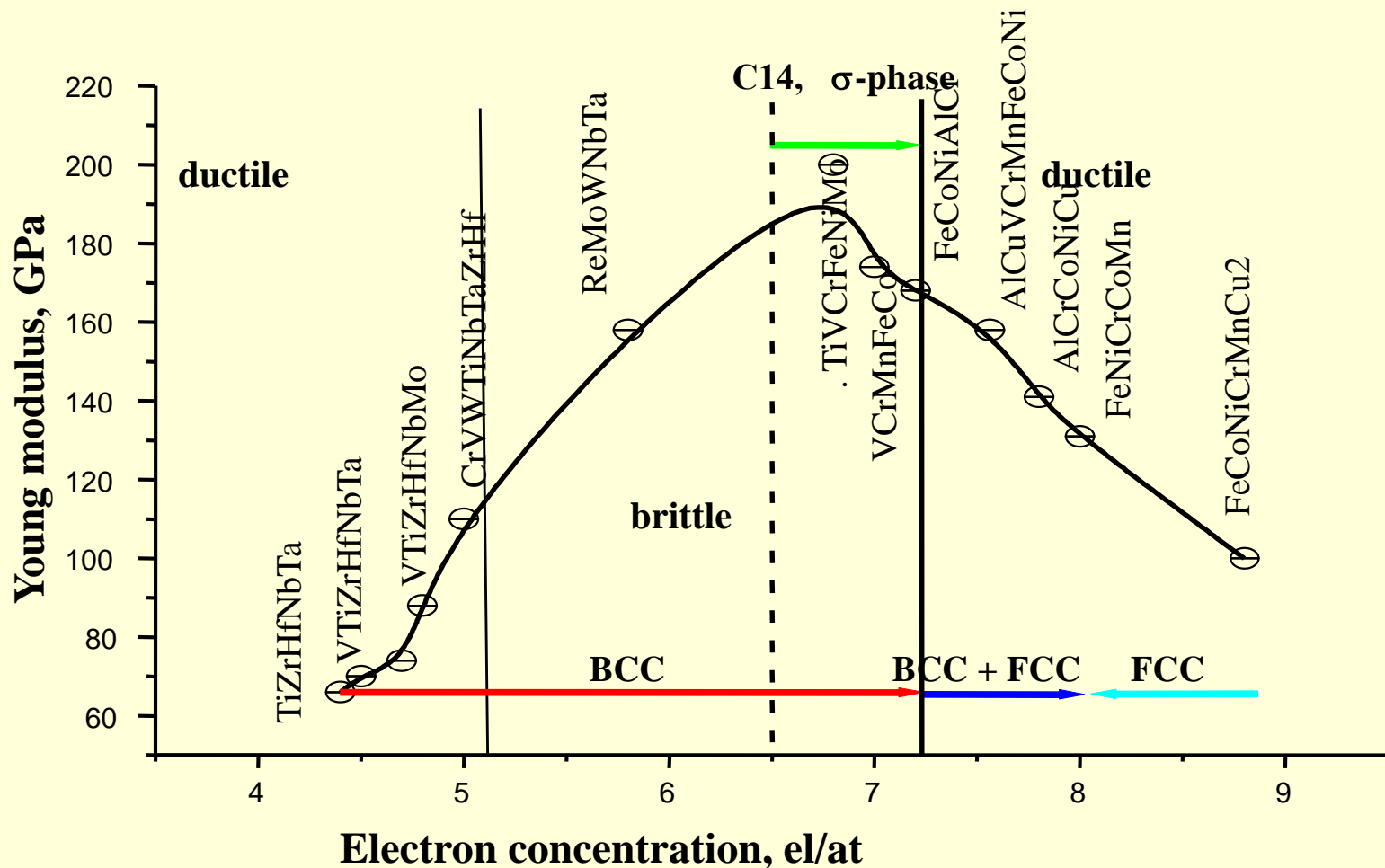
FCC,BCC and FCC+BCC phases versus VEC, ΔH , Δr and Ω



FCC-black points
BCC-red points
FCC+BCC - blue

ΔH - mixing enthalpy
 Δr - atom size difference
VEC- electron concentration

Electron concentration, phase composition and Young modulus of HEA solid solution

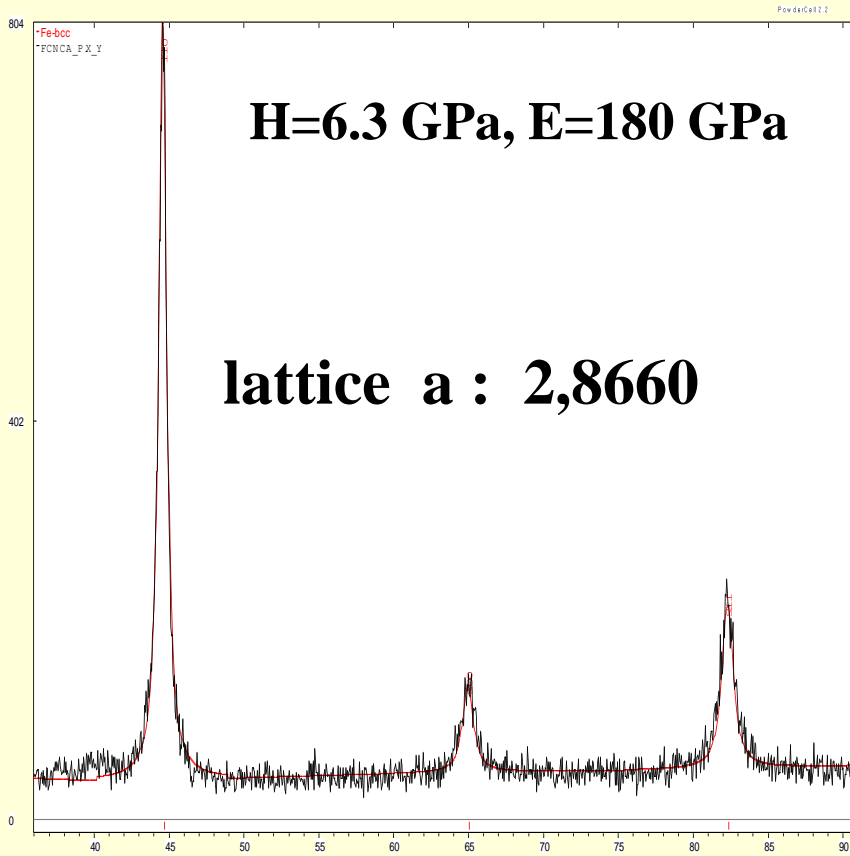


Interrelation between properties of high entropy equiatomic BCC alloys

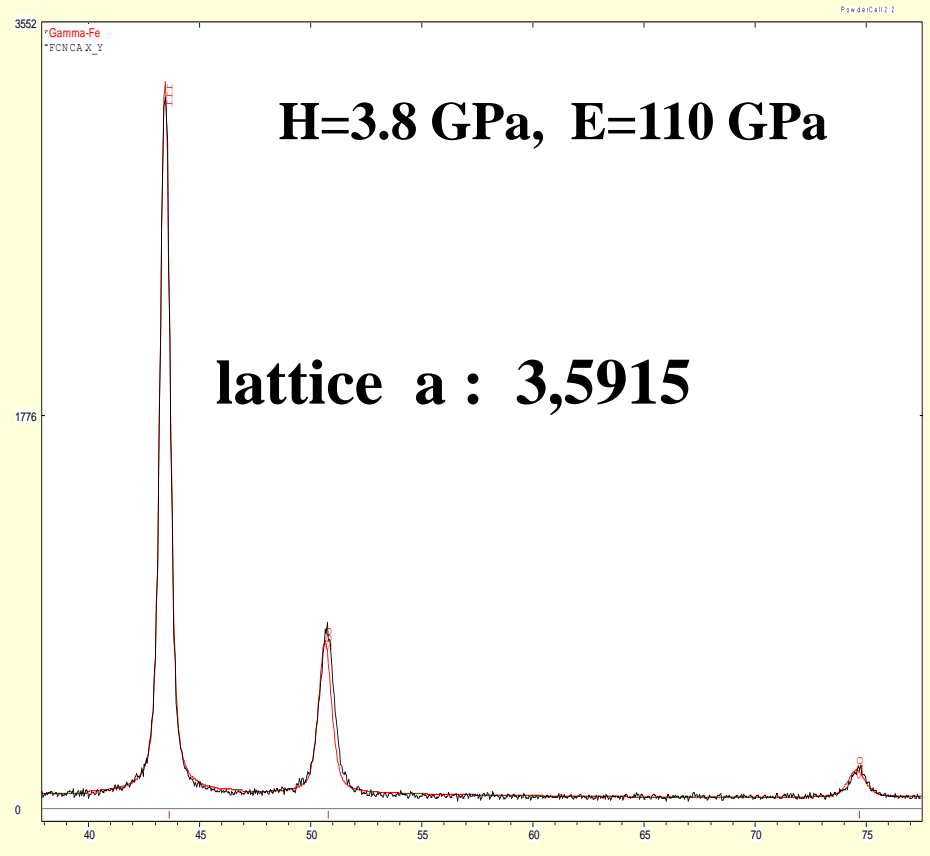
<i>Material</i>	<i>Electron concentration, e/a</i>	<i>E, GPa</i>	<i>a, nm</i>
Fe-Co-Ni-Al-Cr	7.2	168	0.2886
Cr-Fe-Co-Al-Ni-Mn	6.6	130	0.2906
V-Nb-Ta-Cr-W	5.4	100	0.3207
Ti-V-Zr-Nb-Hf	4.6	90	0.3350
Ti-Zr-Hf-Nb-Ta	4.4	88.	0.3352
Ti-Zr-Hf-V-Nb-Ta	4.25	85	0.3405

Structure peculiarities

BCC and FCC equimolar alloys

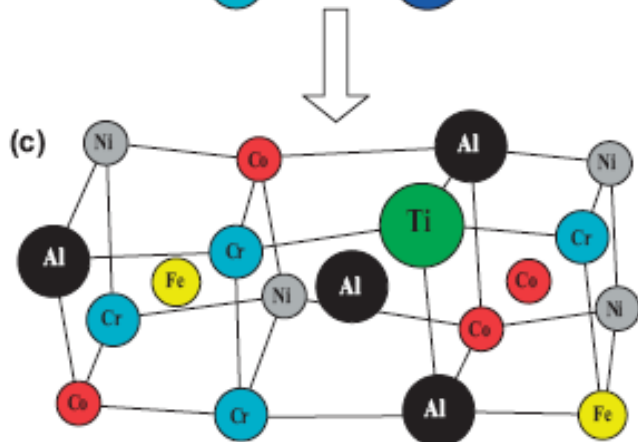
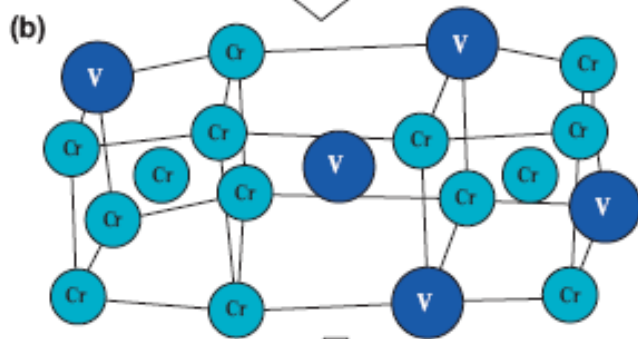
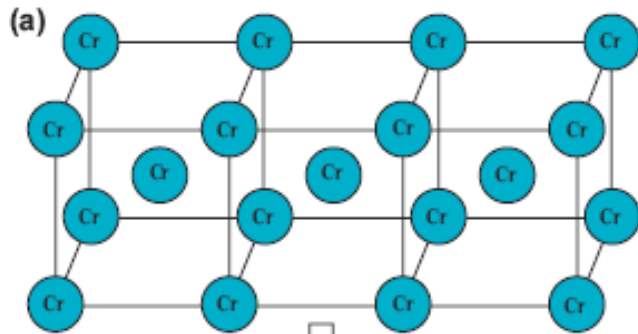


FeCoNiCrAl (BCC), a = 0.2866 nm



FeCoNiCr+0.3Al (FCC), a = 0.3591 nm

BCC structure



(a) – ideal lattice (Cr);

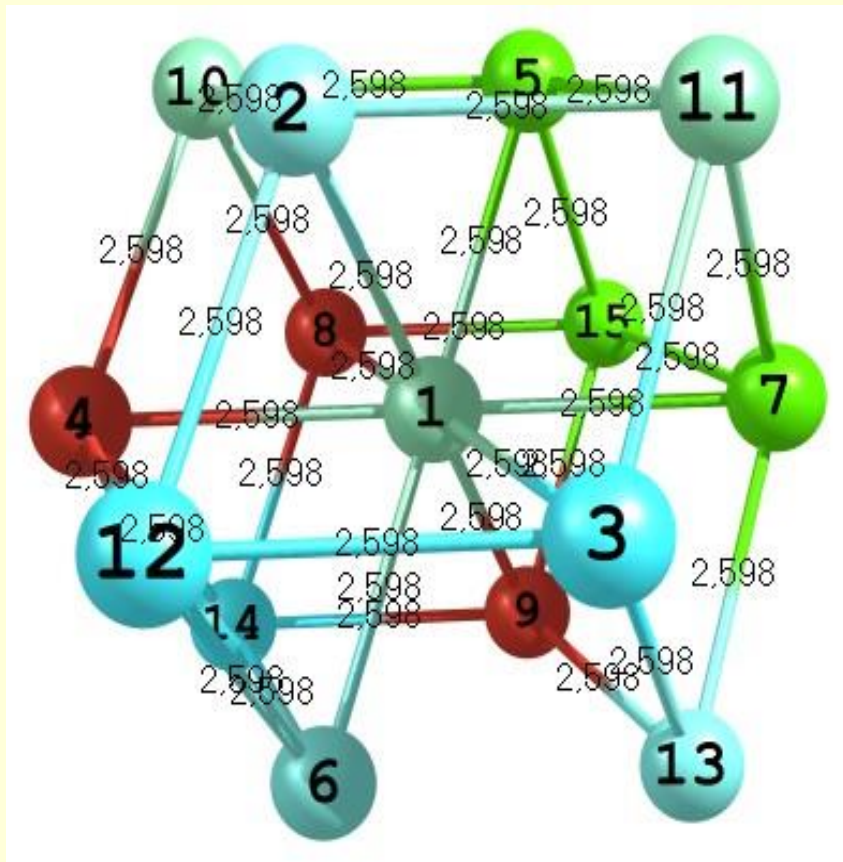
(b) – distorted lattice (Cr-V solid solution);

(c) – extremely distorted lattice in multi-component alloy (CoCrFeNiTi_{0,5})

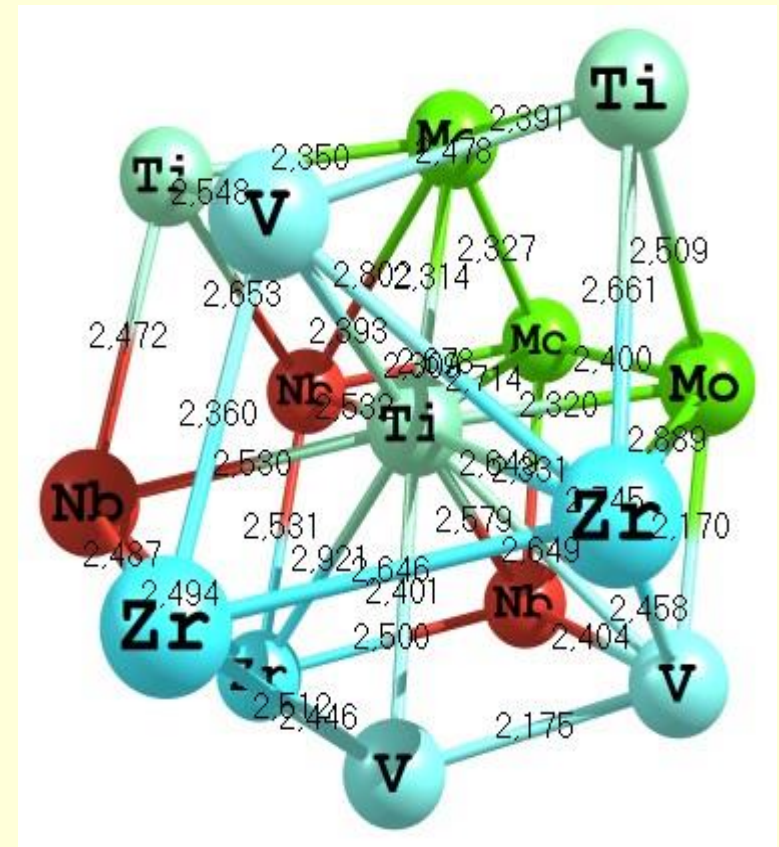
Y. Zhang, Y.J. Zhou, J.P. Lin, G.L. Chen, P.K. Liaw Solid-Solution Phase Formation Rules for Multi-component Alloys // Advanced Engineering Materials, 2008, P. 534–538

Initial (a) and optimized (b) clusters in equiatomic TiVZrNbMo alloy - modeling

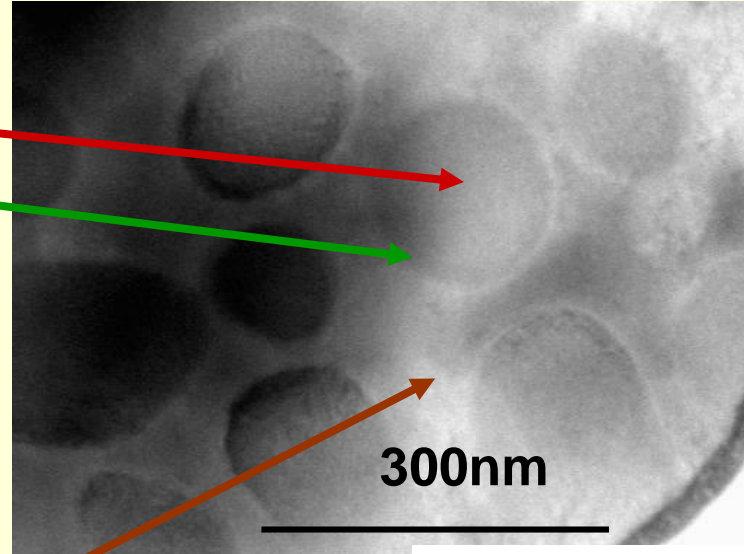
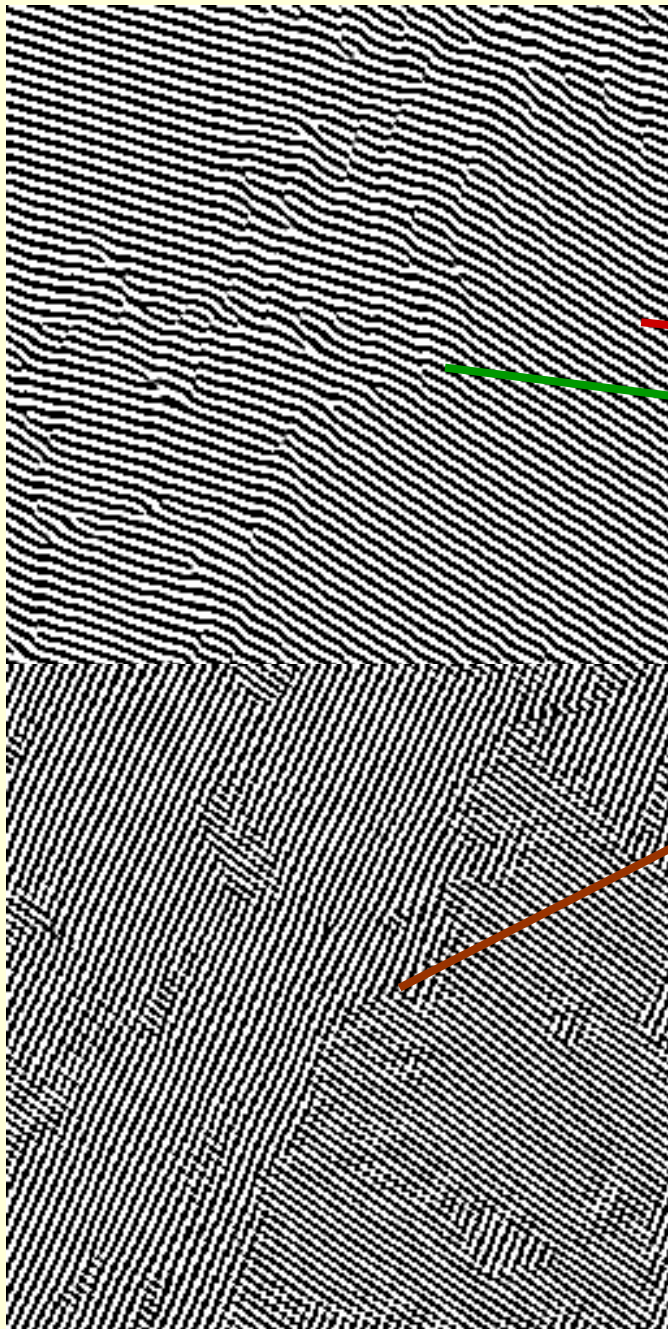
a



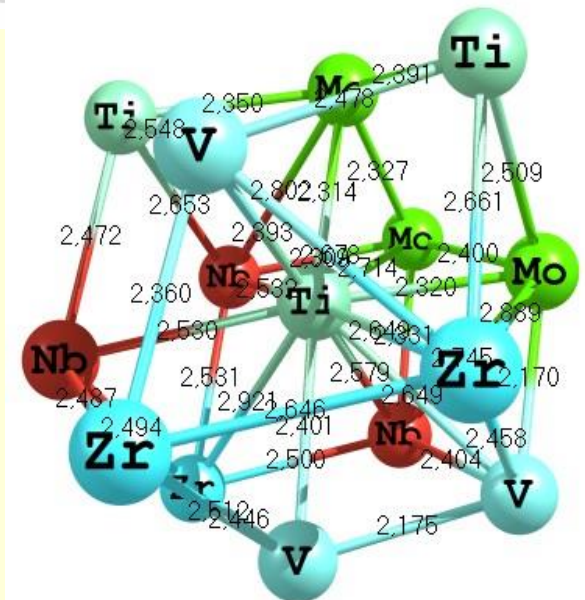
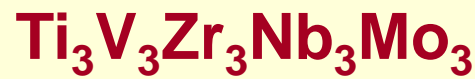
b



Cluster structure of high-entropy alloys

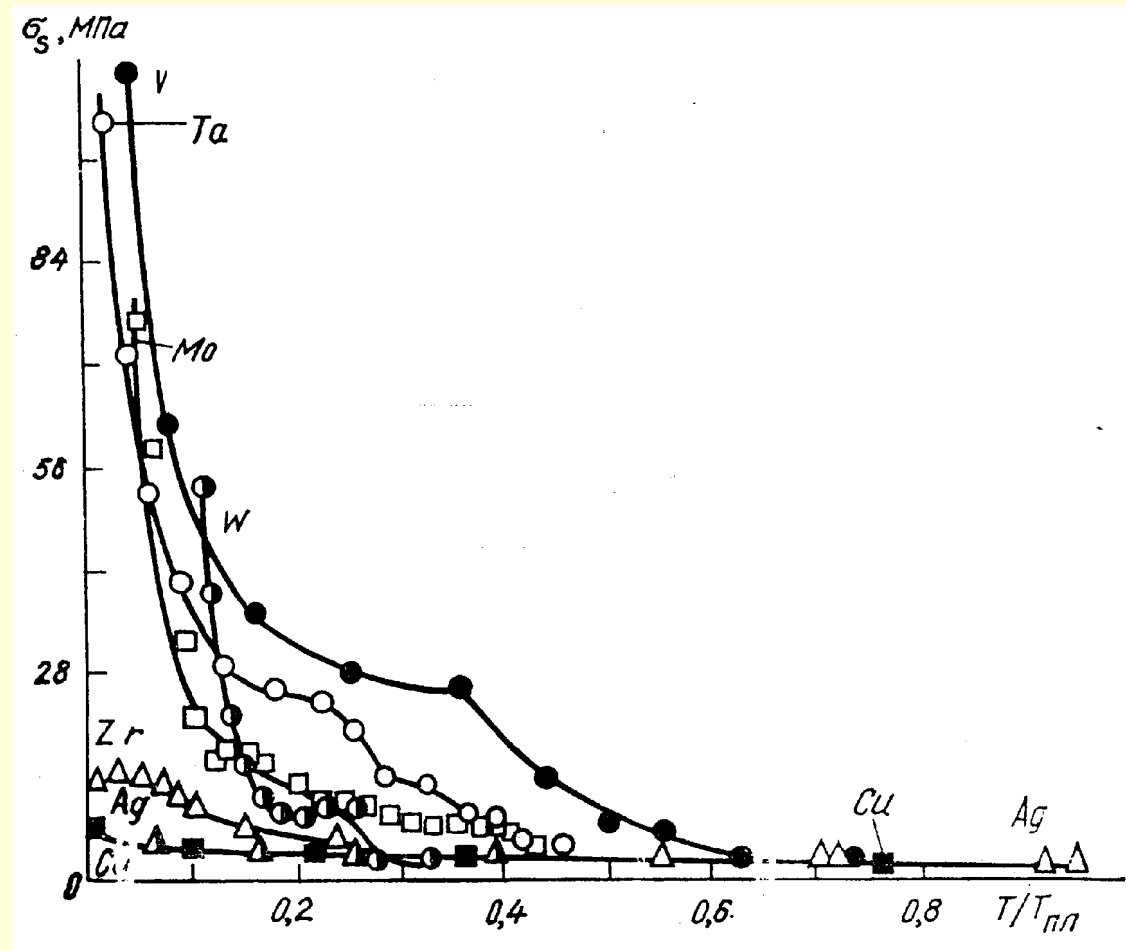


Electron Image 1



***Non-obvious solid solution
hardening***

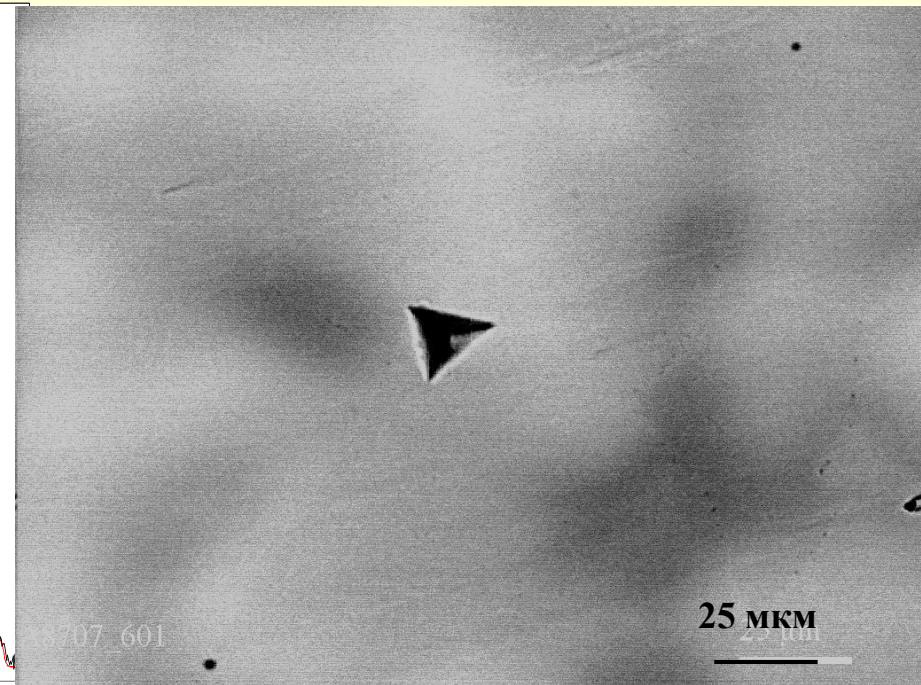
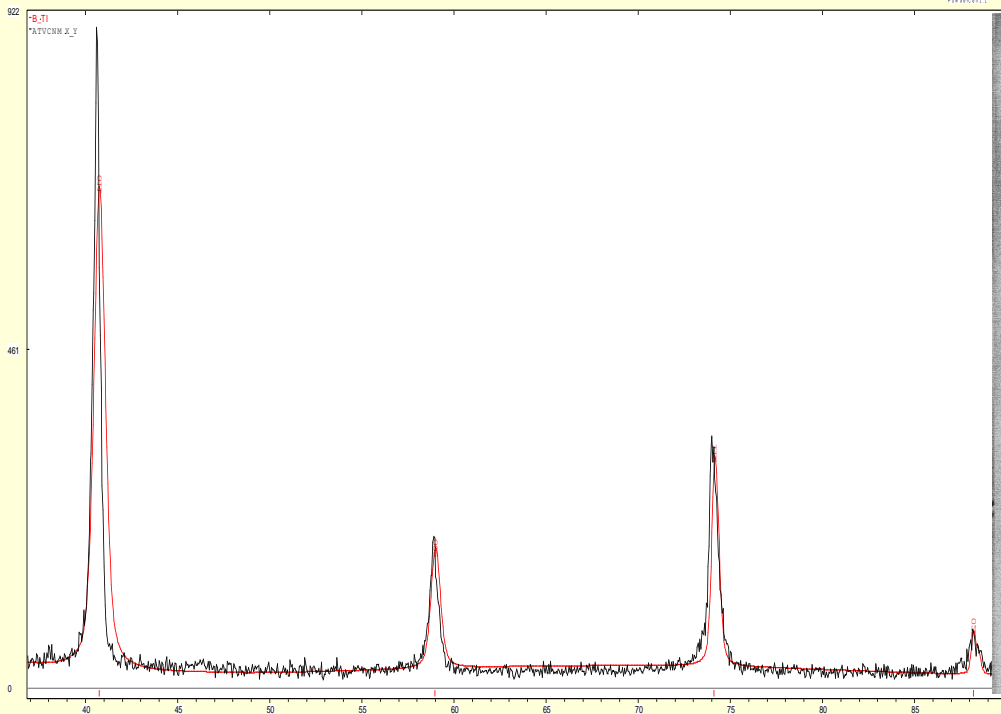
Yield stress temperature dependencies BCC and FCC metals



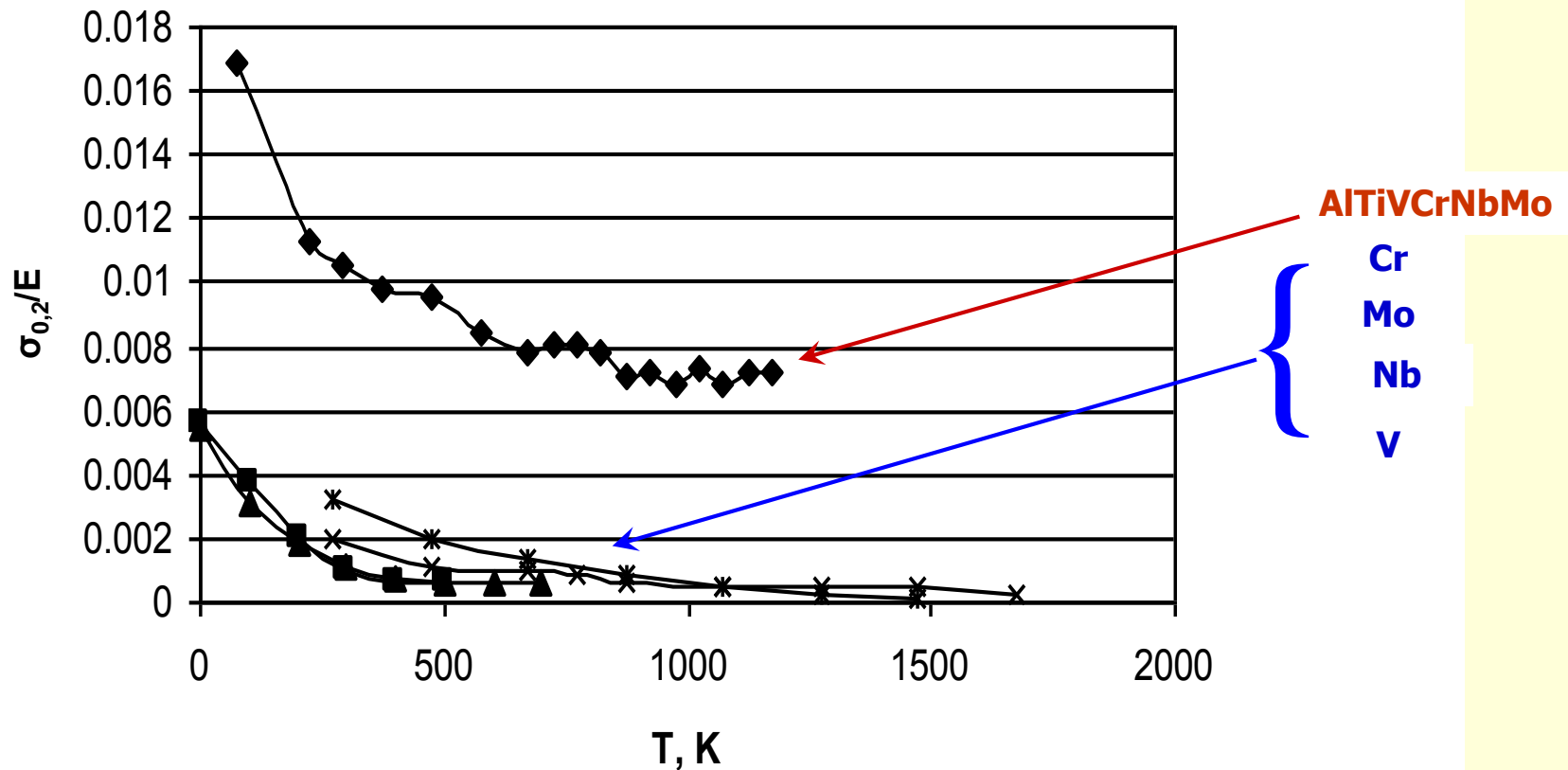
Al-Ti-V-Nb -Cr-Mo (lattice– BCC; $a=0,31307$ нм)

$\Delta S_{\text{mix}}=14,9 \text{ J}\cdot\text{mole}^{-1}\cdot\text{K}^{-1}$; $H_{\text{IT}}=8,1 \text{ ГПа}$; $E^*=160 \text{ ГПа}$

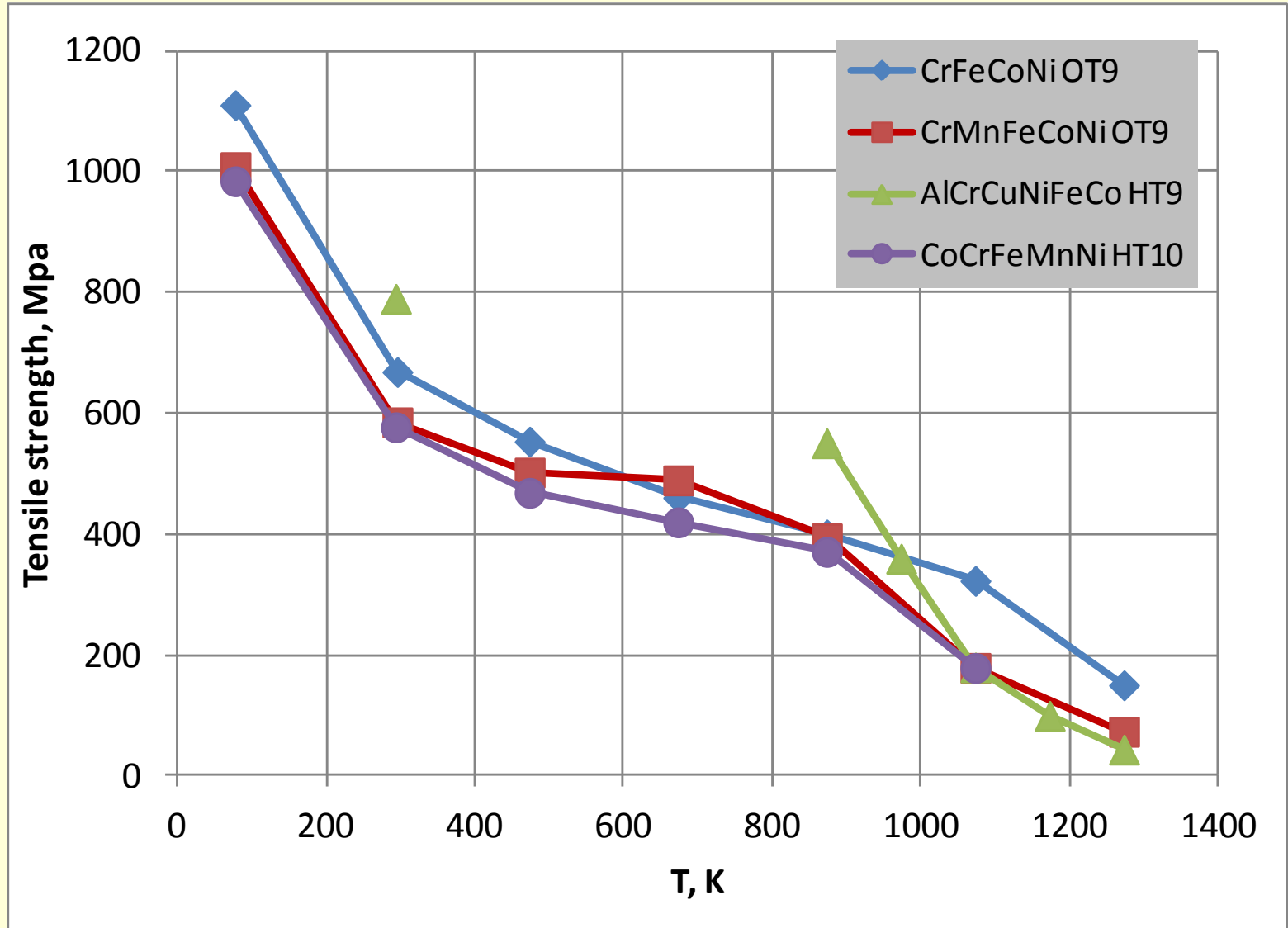
Unusual (non-obvious) hardening
 $\tau=G\Delta a/a$



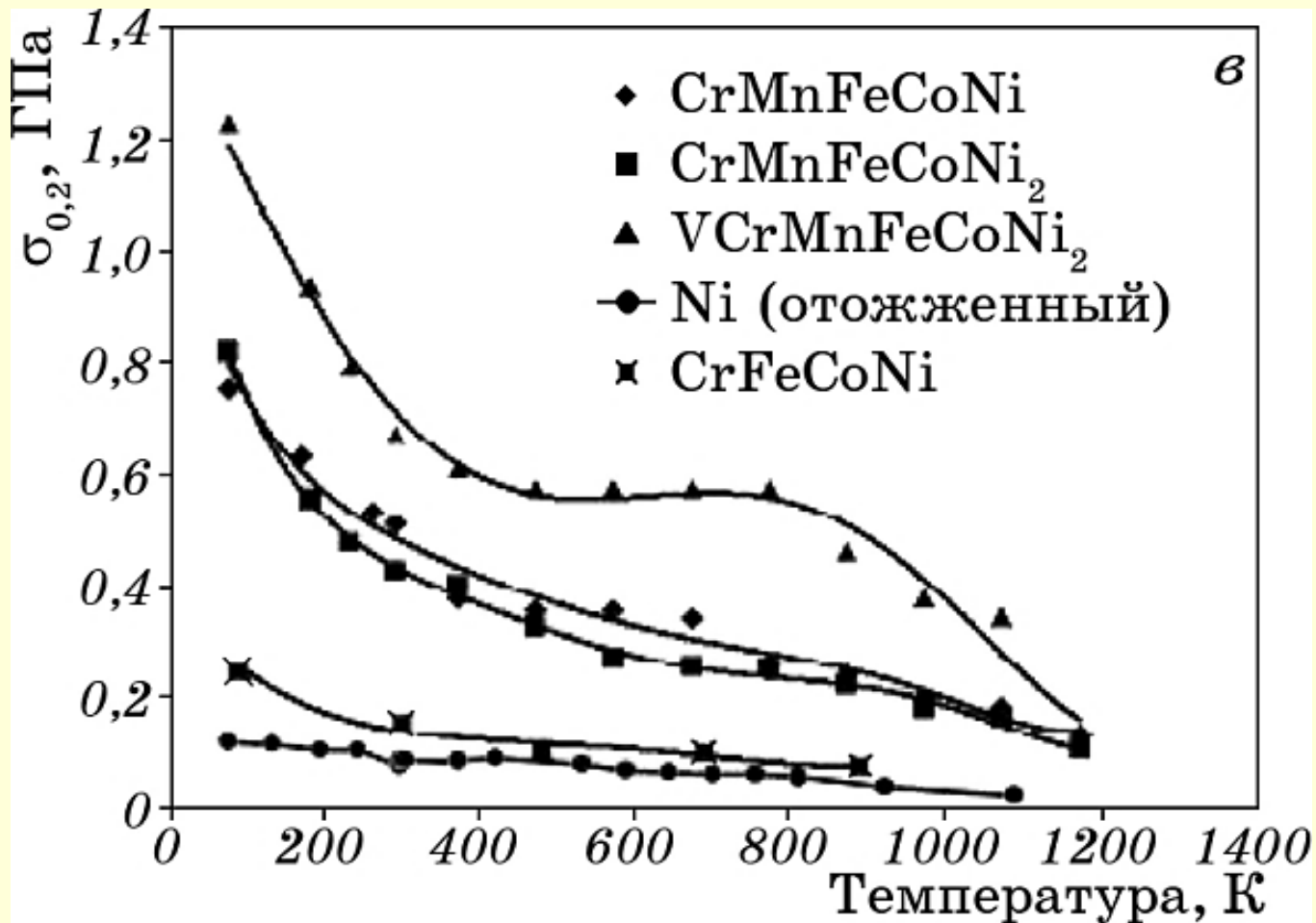
Temperature dependencies of normalized yield stress ($\sigma_{0.2}/E$) for AlTiVCrNbMo alloy and typical BCC metals



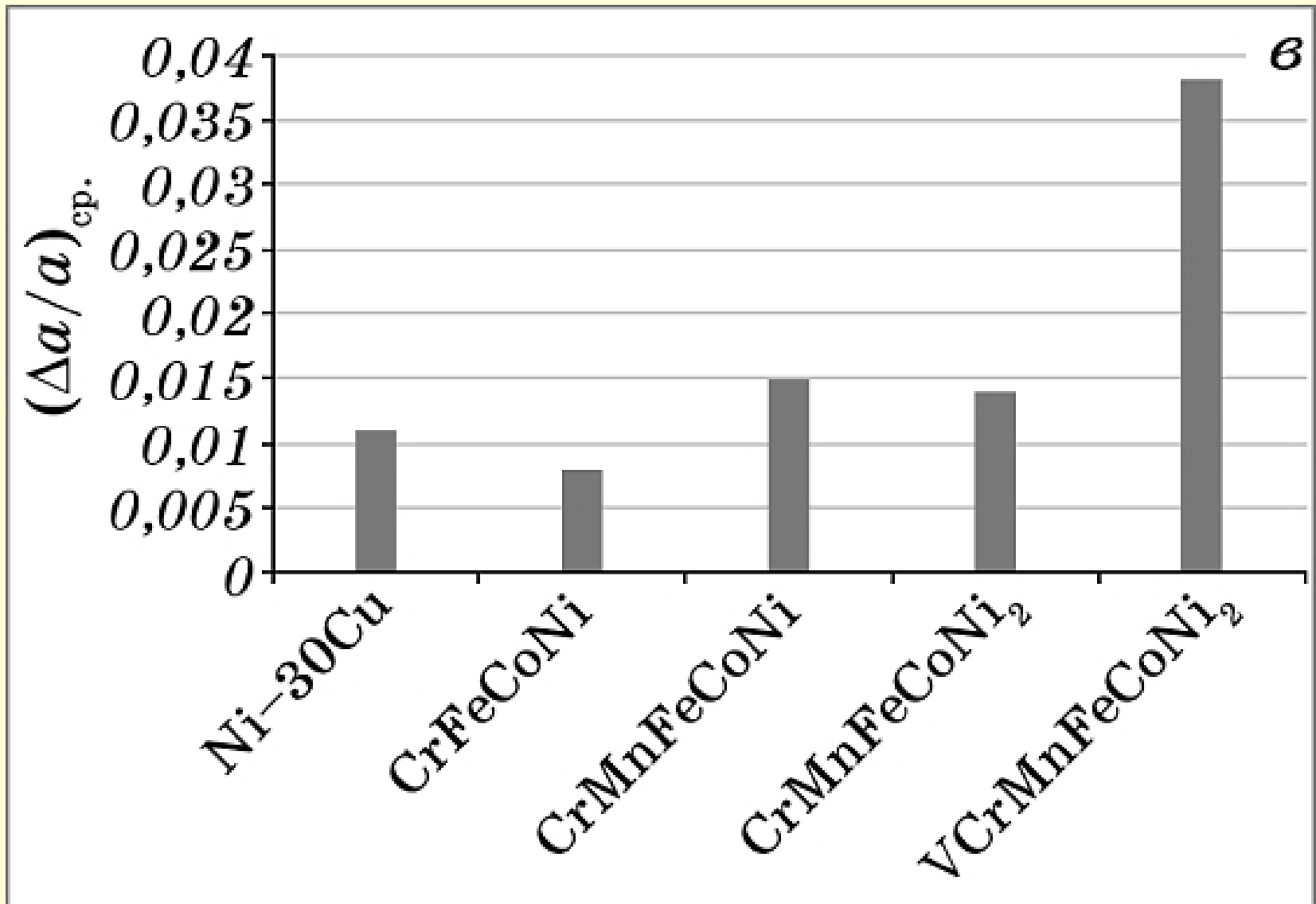
BCC-like behavior in FCC HEAS



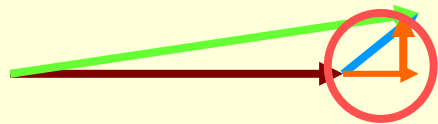
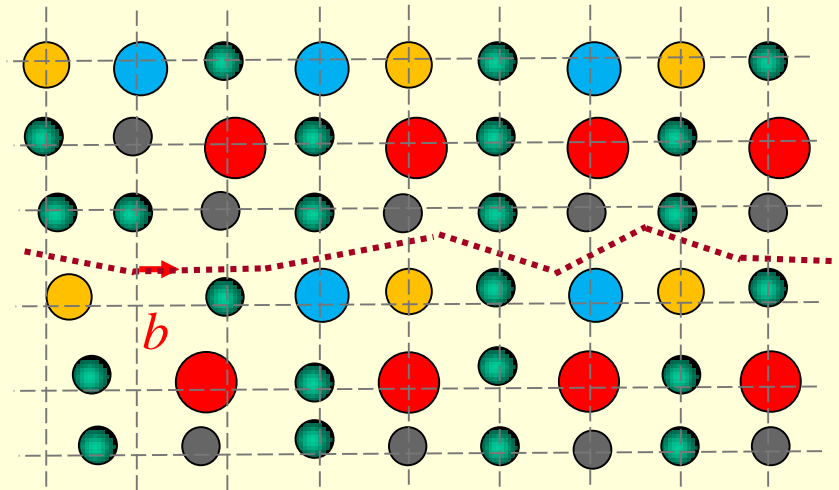
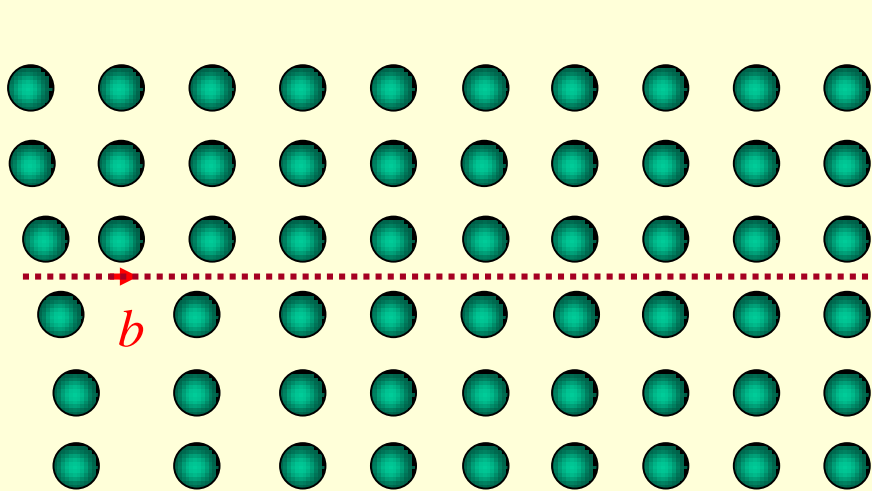
BCC-like behavior in FCC HEAS



Average lattice distortion



Single dislocation movement in some pure metal and HEA



$$\vec{b} = \vec{b}_0 + \vec{\Delta b}$$

Burgers vector precession!

$$\Delta\tau = k(\overline{\Delta b/b})G$$

Hardening due to lattice distortions

$$\Delta b_n = 0,5b(\Delta a/a)$$

$$\Delta\sigma = 0,5(\overline{\Delta a/a}) G$$

$$\Delta H = k_H(\Delta a/a)G,$$

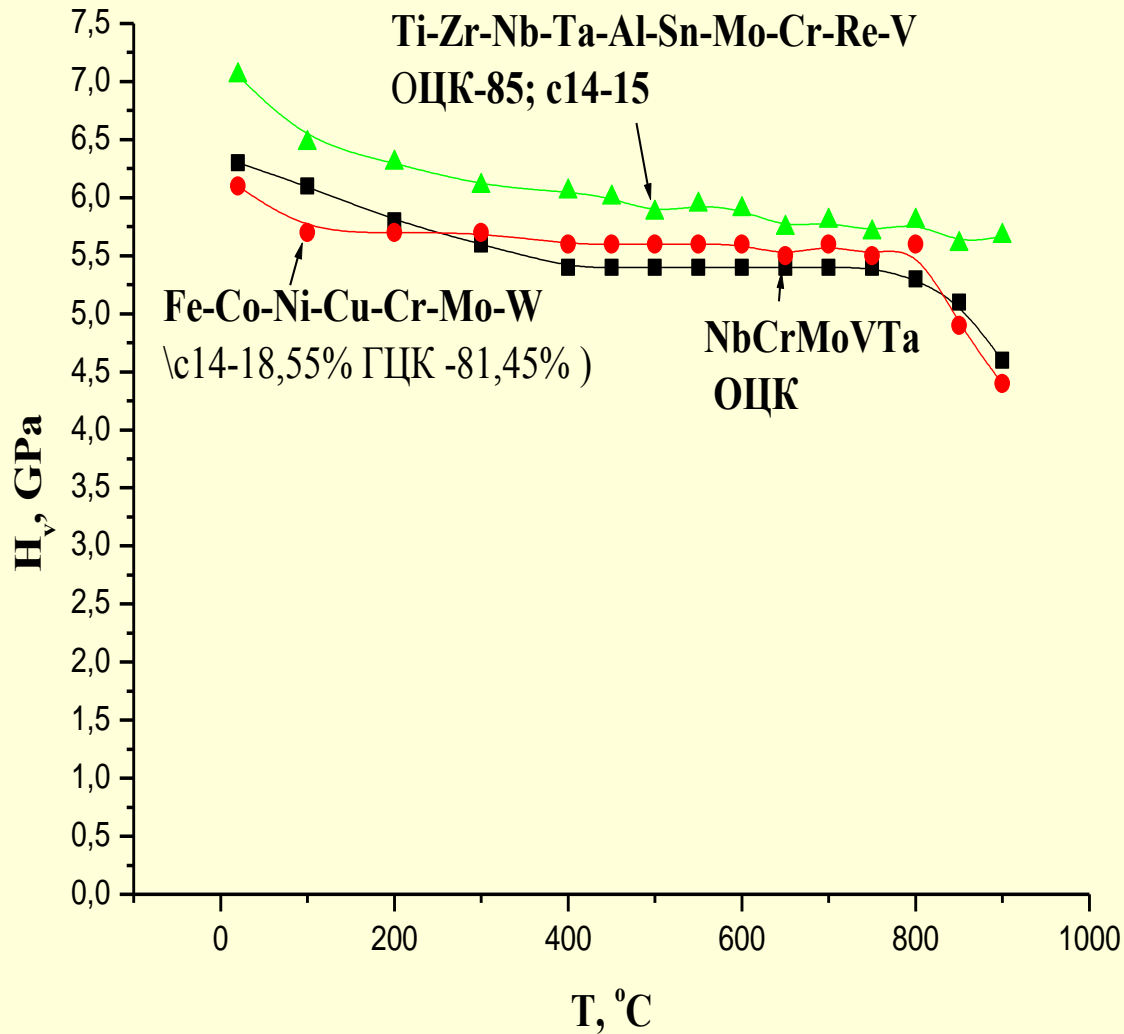
$$H = H_{\text{mix}} + \Delta H = H_{\text{mix}} + k_H(\Delta a/a) G$$

$$k_H \approx 1,5$$

Hardening parameter K_H

Alloy	Lattice parameter, nm	Hardness, GPa	K_H
AlCrMoNbVTi	0,3128	5.1	1,57
TaNbHfZrTi (D.Miracle)	0,3404	3,826	1,59
WNbMoTaV (D.Miracle)	0,3183	5,25	1.51

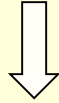
Hot hardness dependence upon temperature for selected HEA`s



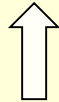
Reasons for athermal “plateau”

- Pico-level lattice distortions
- Peculiarities of GB – engineering in HEAs (healing of weak places in GB)
- Possible DSA effects in multi-component alloys

Boundary



M-M-M-M=M-M-M-M
M-M-M-M=M-M-M-M
M-M-M-M=M-M-M-M
M-M-M-M=M-M-M-M
M-M-M-M=M-M-M-M
M-M-M-M=M-M-M-M



M-M-M-M=M-M-M-M
M-M-M-M=**X**-M-M-M
M-M-M-**X**=M-M-M-M
M-M-M-M=**X**-M-M-M
M-M-M-**X**=**X**-M-M-M
M-M-M-M=M-M-M-M



If $E_{xx} > E_{MM}$ and $E_{MX} > E_{MM}$ strength (hardness) increases.

If $E_{xx} (E_{MX}) < E_{MM}$ strength (hardness) decreases.

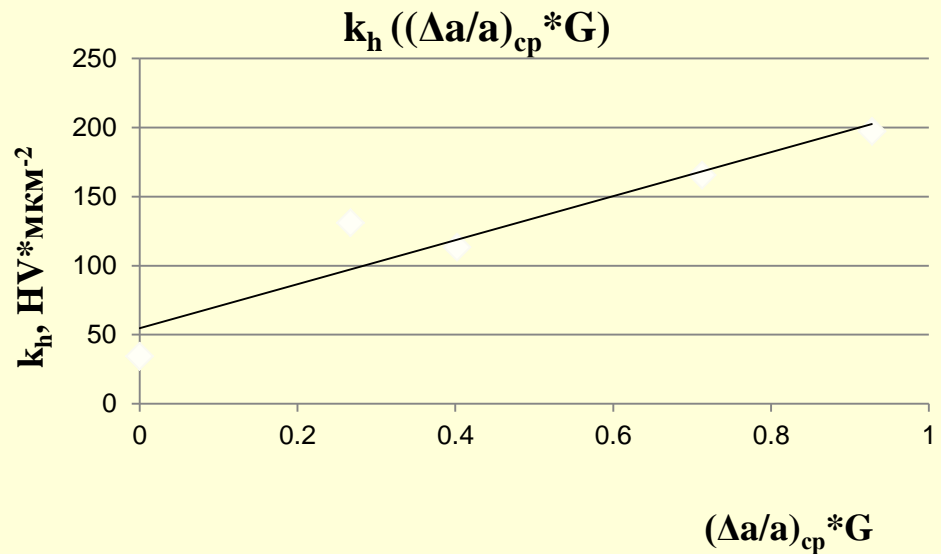
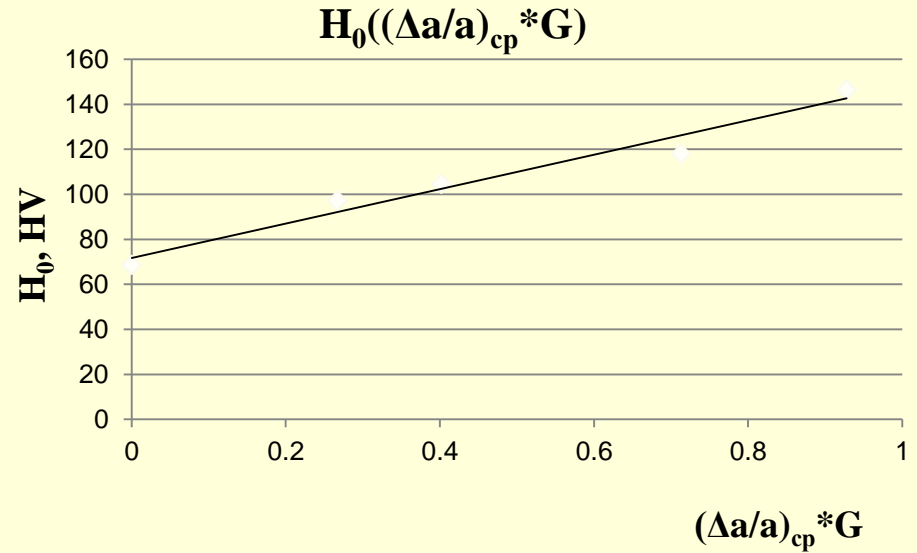
In multicomponent systems the possible **healing of the weak points** in the grain boundaries structure can occur and this can lead to the extremely high strength (hardness). Using the **segregation of the useful impurities** or alloying elements, it is possible to realize the **healing of weak places in the grain boundaries** and to **obtain the essential increase of mechanical properties as a result.**

Distortion effect on parameters H_0 and k_H in equation

$$H = H_0 + k_H d^{1/2}$$

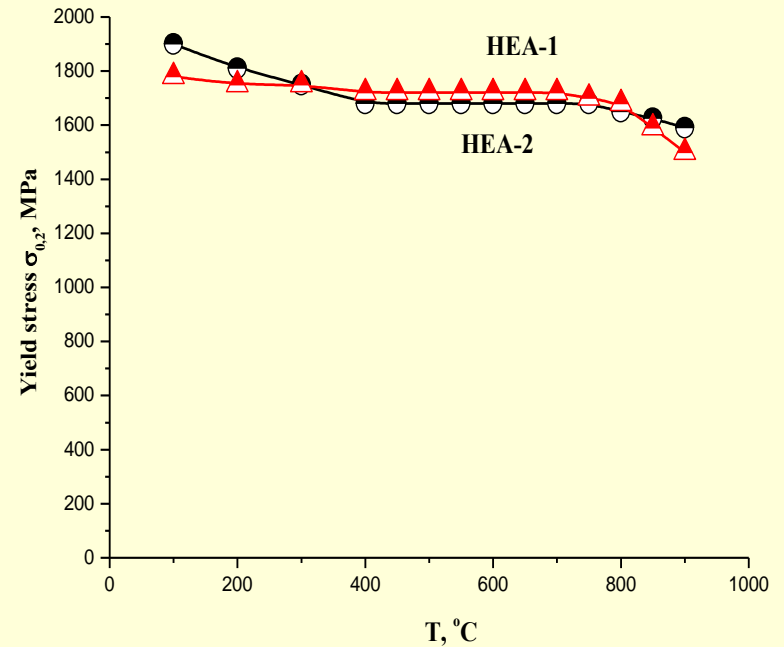
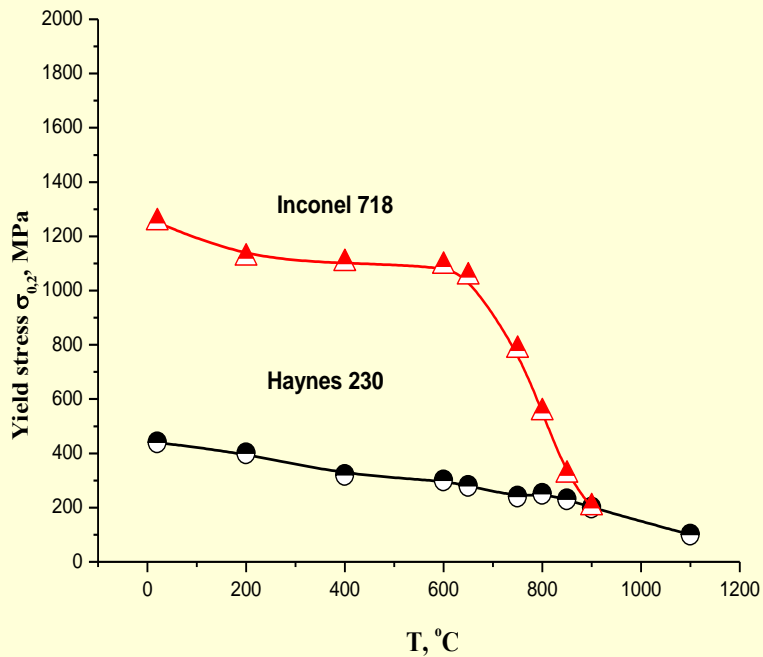
Alloy	Hall-Petch intercept, H_0 (HV)	Hall-Petch slope k_H (HV· μm^{-2})
FeNiCoCr	118	165.5
FeNiCo	97.3	131.1
NiCoCr	146.5	197.3
FeNi	104.7	113.4
NiCo	62.2	167.1
Ni	68.6	34.3

[Wu, Zhenggang, "Temperature and Alloying Effects on the Mechanical Properties of Equiatomic FCC Solid Solution Alloys. " PhD, diss., University of Tennessee, 2014. P. 125. http://trace.tennessee.edu/utk_graddiss/2884]



$$(\Delta a/a_B)_{cp} = \sum c_i (a_i - a_B) / a_B$$

Yield stress temperature dependencies



Inconel 718, Haynes

HEAS, IPMS

Now we are working with two alloy groups with decreased density

- Density 6 - 8 g/cm³ instead 8.5-9 g/cm³ g/cm³ (materials competitive with Inconel and Haynes)
- Density 3.6 -3.9 g/cm³ instead 4-4.5 g/cm³ (materials competitive with γ -aluminides)

T,K	σ_Y , MPa	σ_u	δ , %
273	930	980	10,5
1073	837	810	35
1173	430	450	37
1273	230	250	40
1373	110	120	45

Density 7,9 g/cm³

T,K	σ_Y , MPa	σ_u	δ , %
273	1247	1463	6,8
373	1123	1962	11,2
573	872	1858	10
773	896	1306	14,1
1023	775	837	16,2

Density 3,9 g/cm³



(Nb-Cr-Al-Ti-Zr-Si)

$$\gamma = 6,35 \text{ g/cm}^3;$$

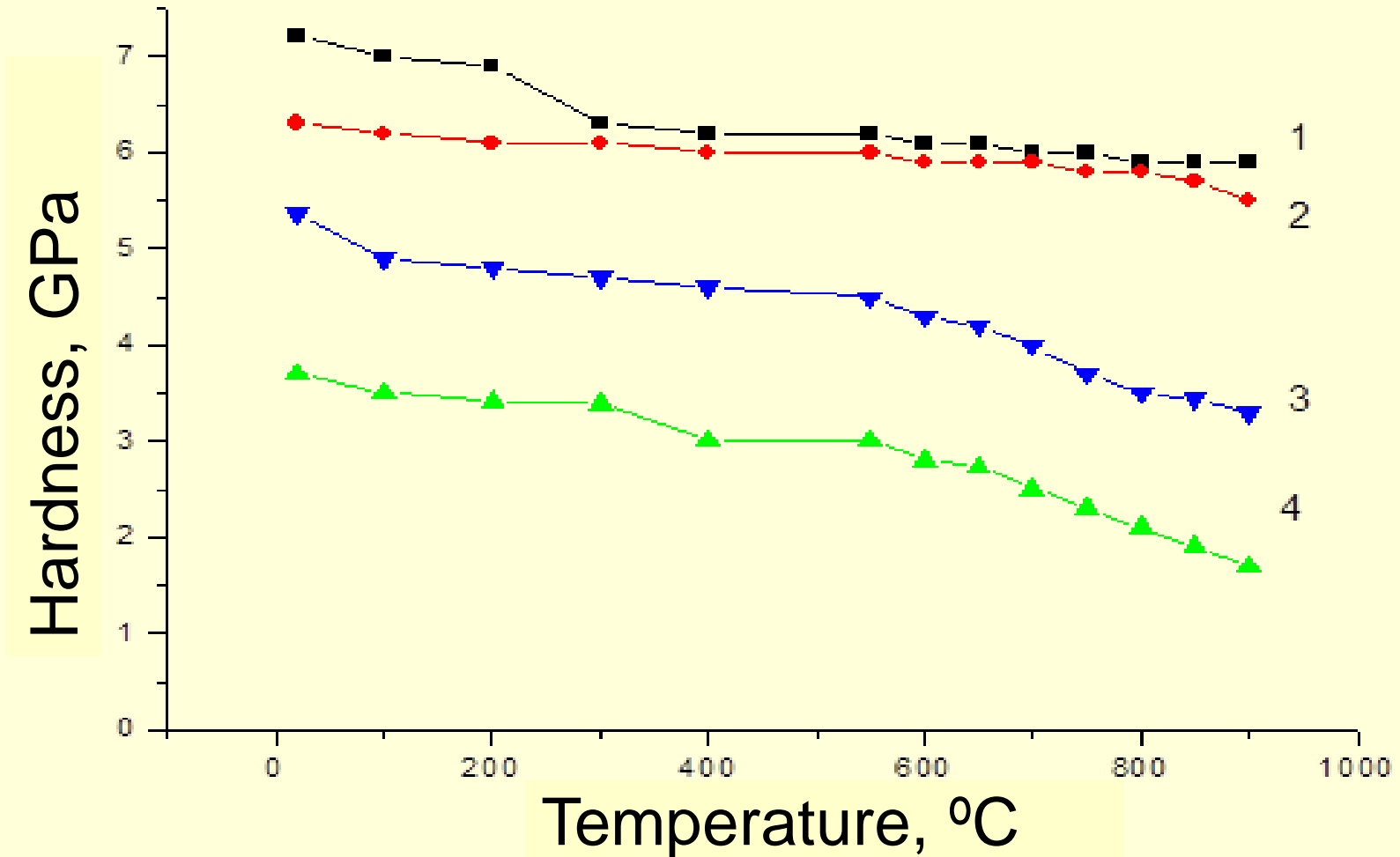
$$T = 1000 \text{ }^\circ\text{C};$$

$$\sigma_{02} = 860 \text{ MPa}$$

Solid solution and phase
type $\text{Me}_3\text{-X}$

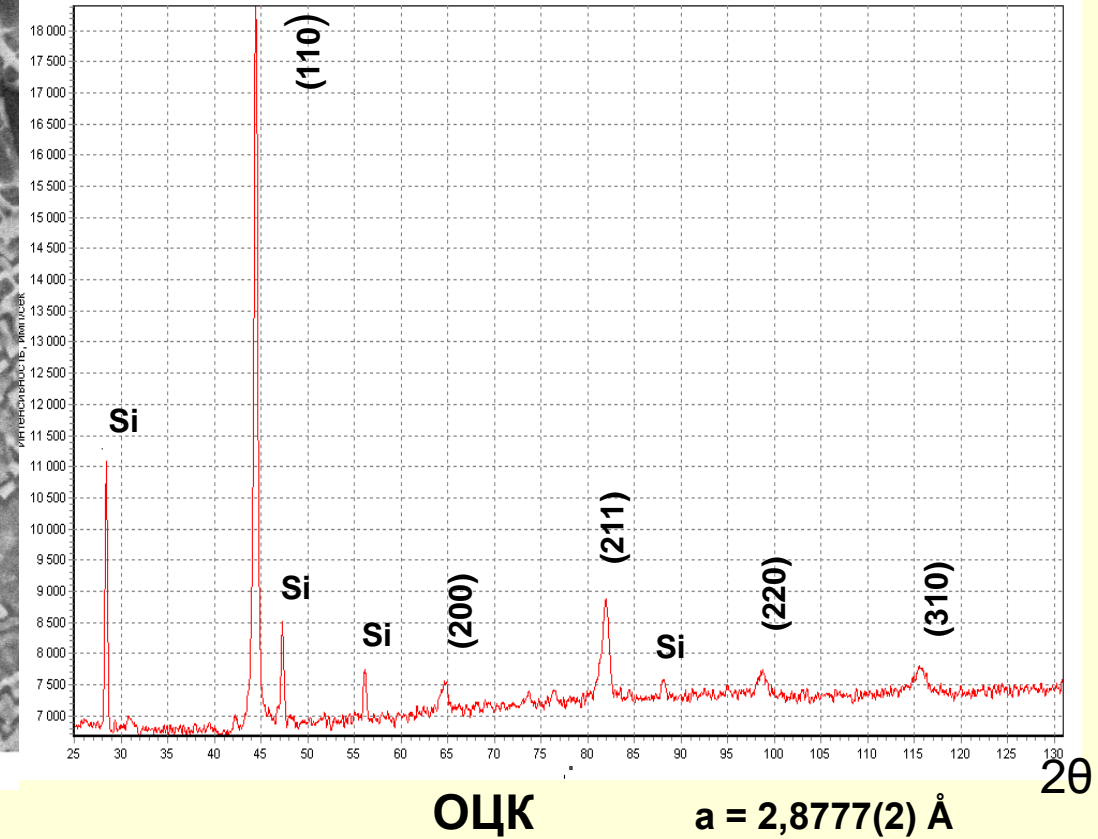
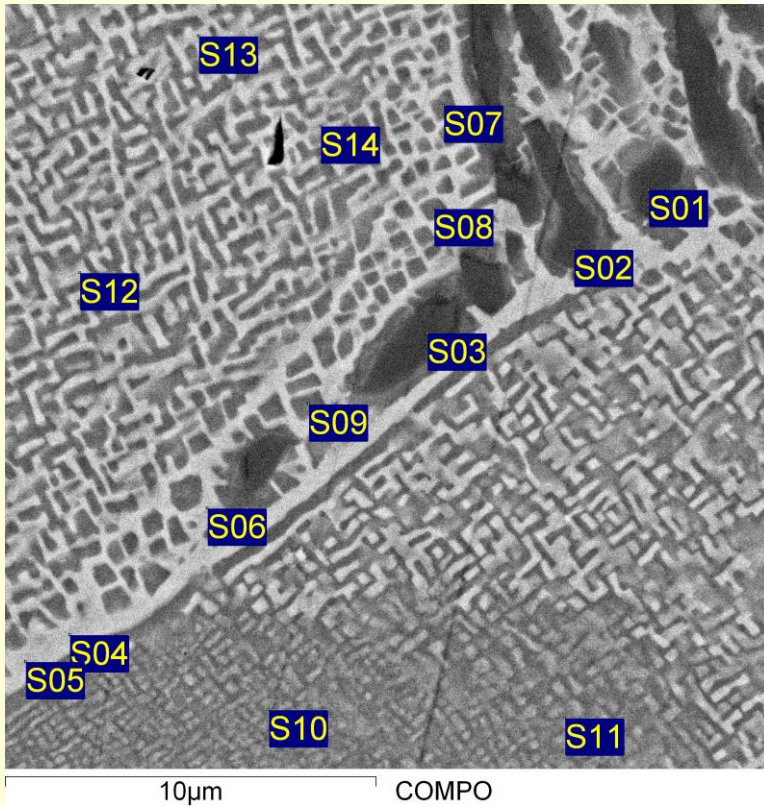
Composites and in-situ composites

High-temperature hardness

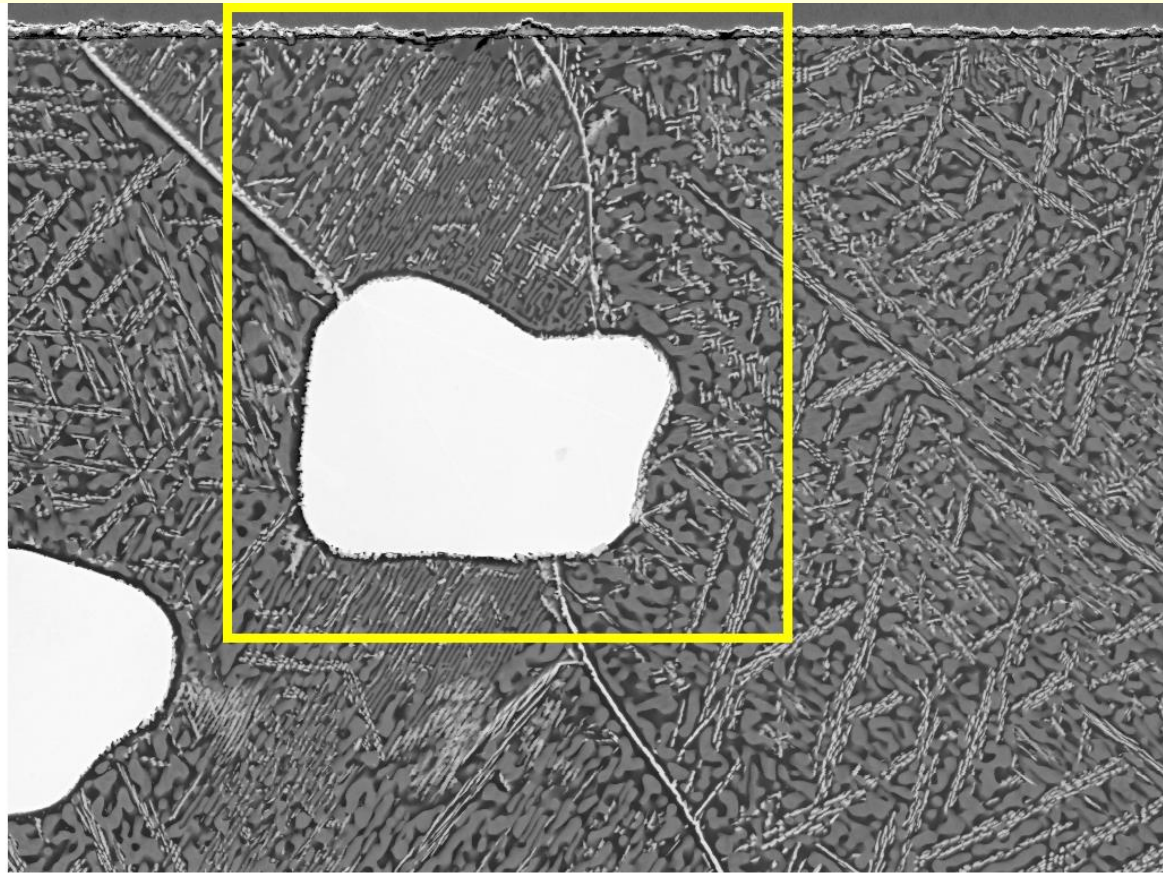


- 1- NbCrMoVTa; 2- FeCoNiCrW;
3- TiZrVNbCr; 4- TiZrHfVNb

Al-Cr-Fe-Cu-Ni



Al CR Fe Co W

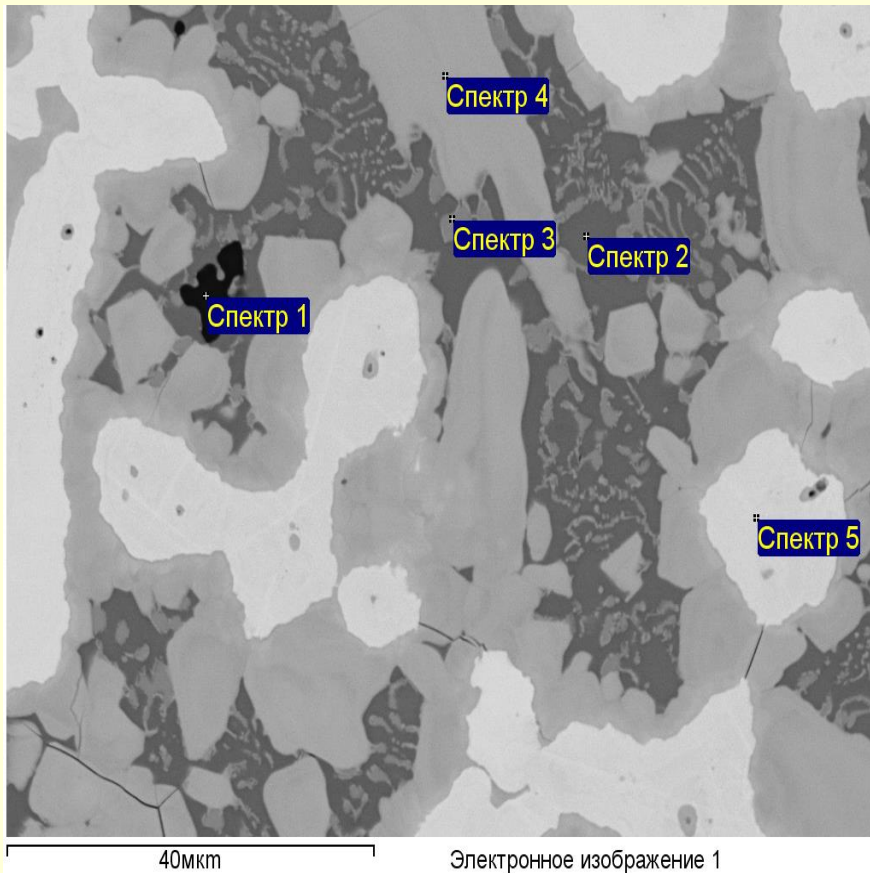


20 μ m

BSE, EHT = 15 kV

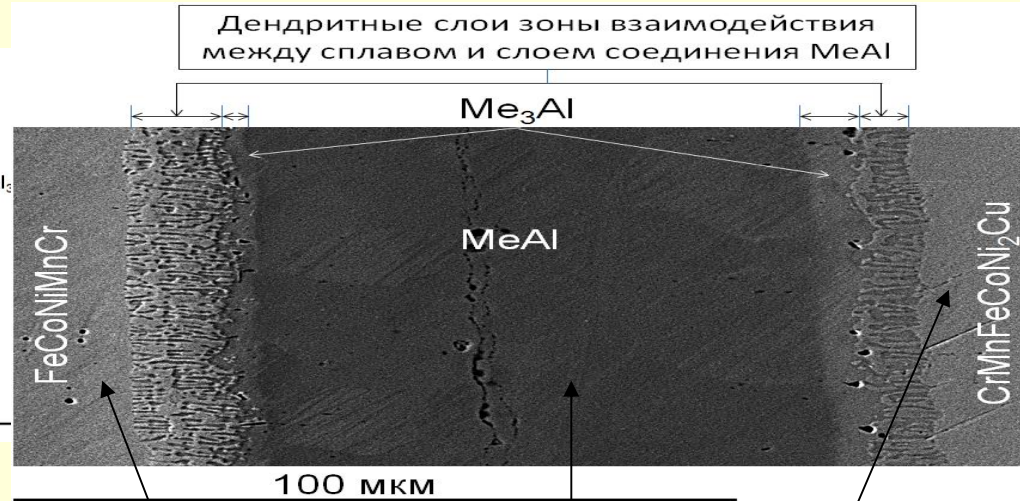
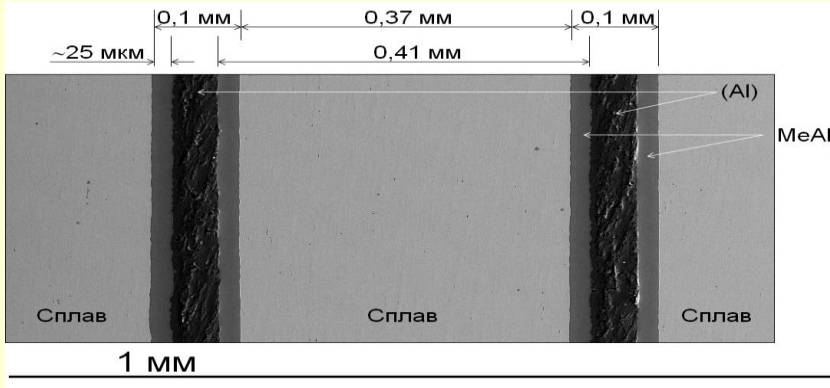
Structure and composition of phases in Fe-Ni-Co-Cr-Mo-W equiatomic alloy

BCC- 45,29 %; $(\text{FeCoNiCr})_3(\text{MoW})_2$ - 40,19 %; FCC- 14,52 %

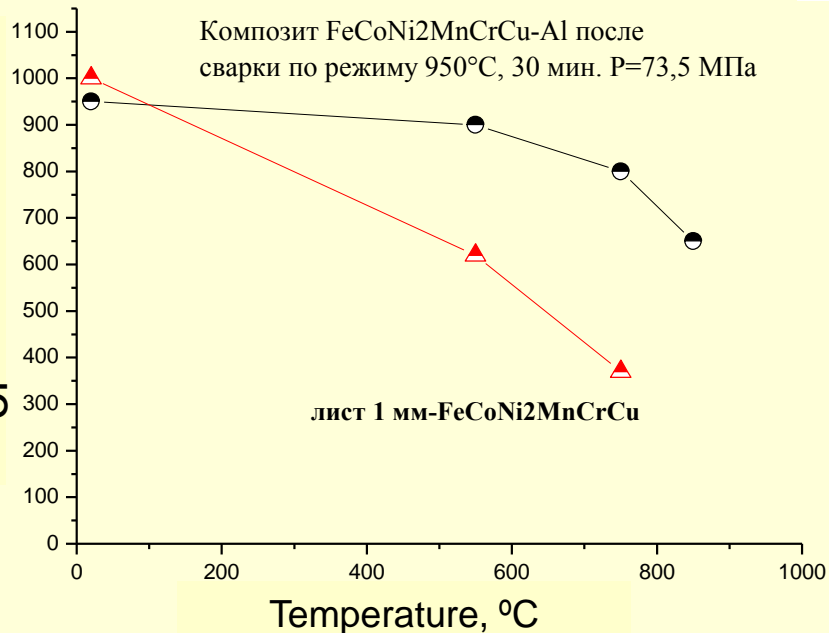


element \	5 BCC	4 HCP	2 FCC
W	59.43	18.87	3.46
Mo	30.43	21.28	8.95
Cr	6.92	15.72	20.30
Fe	2.22	16.10	18.70
Co	1.00	16.22	18.70
Ni	0.00	11.80	25.78

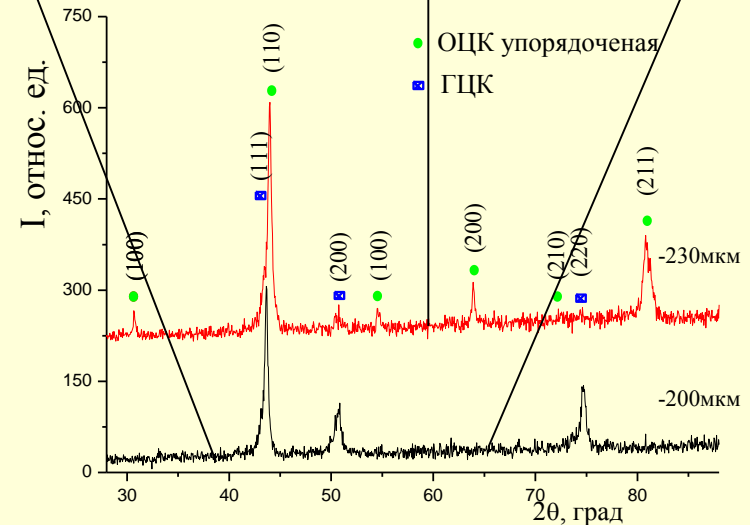
STRUCTURE and PROPERTIES of FeCoNi2MnCrCu-Al Composite



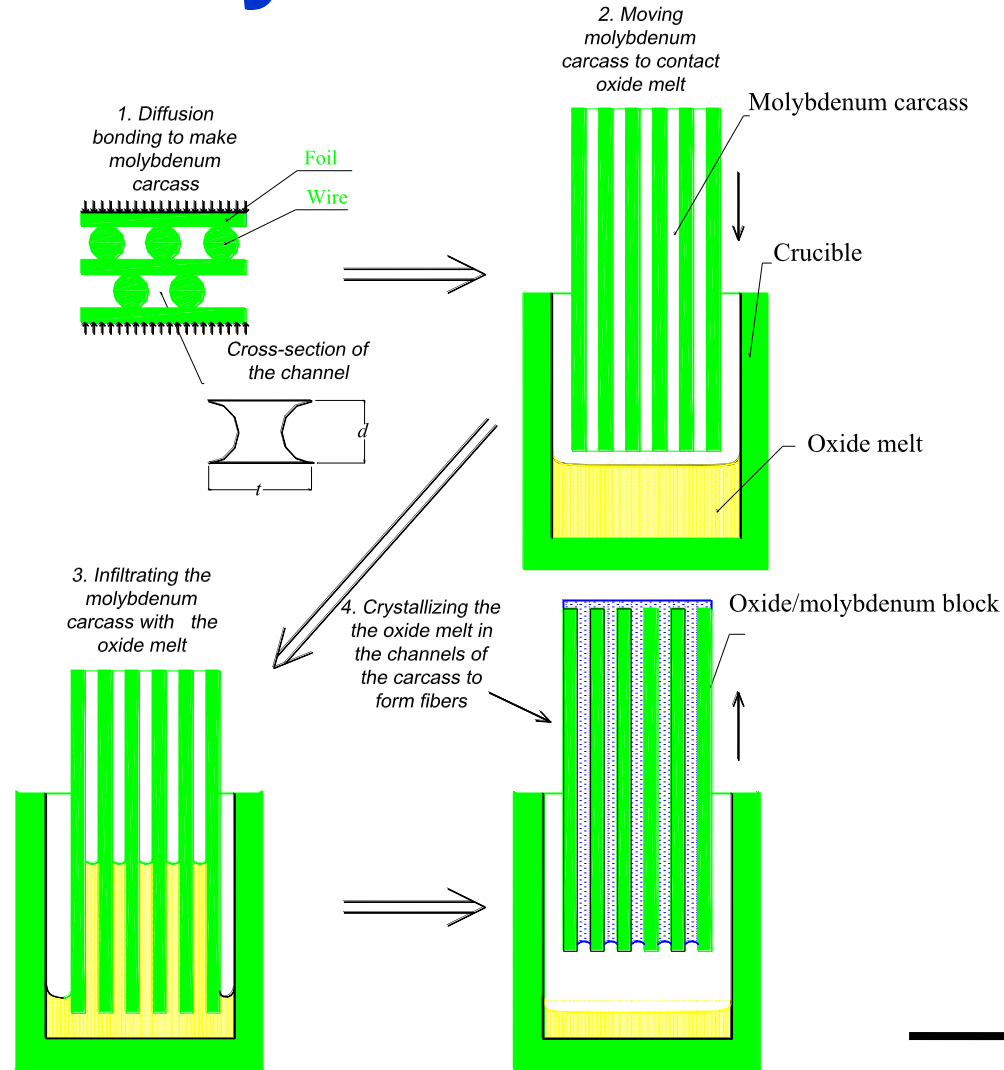
600°C, 2 h, P=7,3MPa



950°C, 30 min, P= 73,5 MPa



Internal crystallisation method

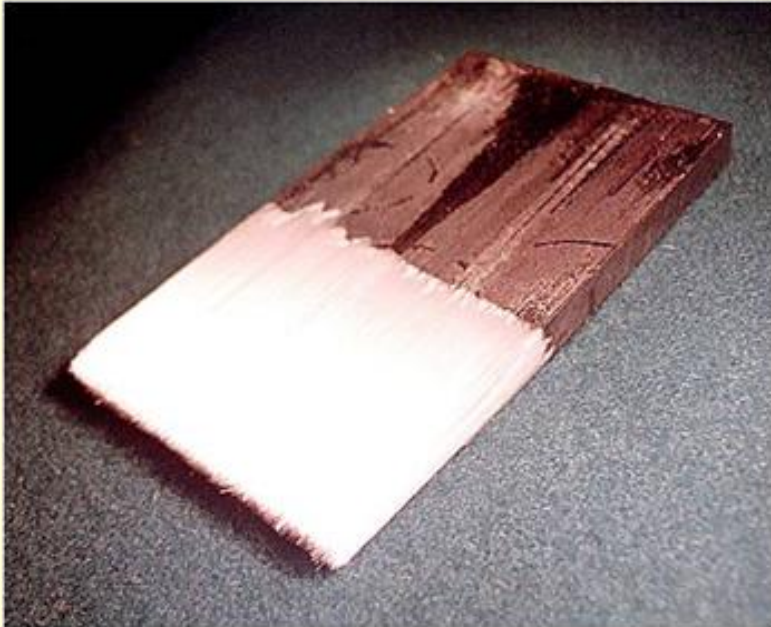


Mileiko ST, Kazmin VI. Crystallisation of fibres inside a matrix: a new way of fabrication of composites. J Mater Sci 1992; 27(8):2165-2172.

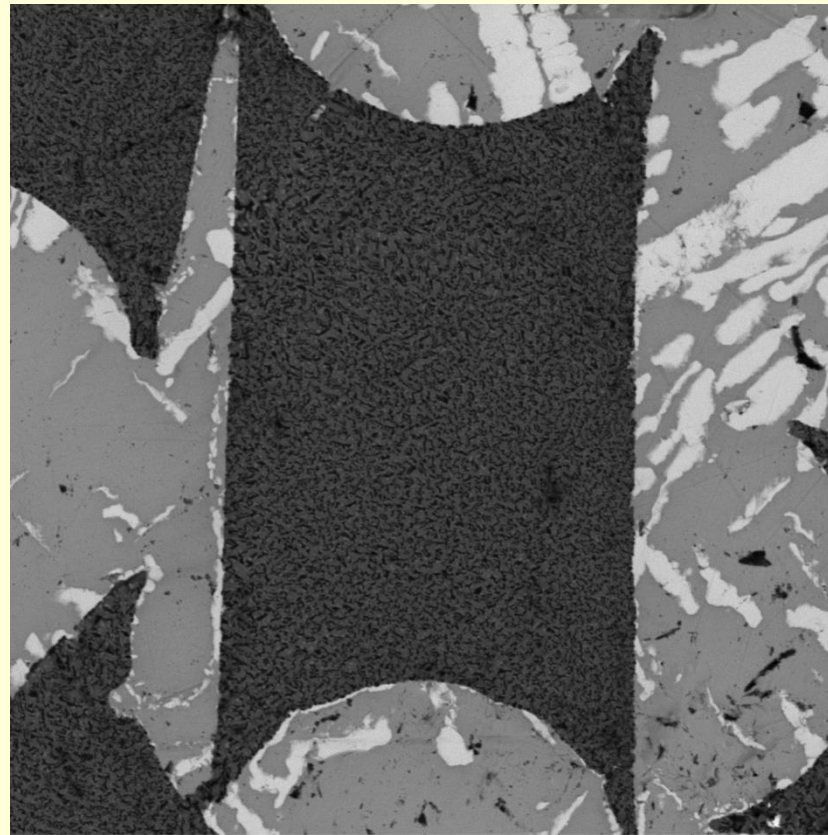
Mileiko ST. Single crystalline oxide fibres for heat-resistant composites. Compos Sci Technol. 2005; 65(15-16):2500-2513.

Internal crystallisation method

5. Dissolution of molybdenum

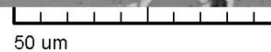


Eutectic fiber $\text{Al}_2\text{O}_3\text{-Y}_3\text{Al}_5\text{O}_{12}\text{-ZrO}_2$ in matrix FeCoNiCrW after treatment at 1530°C .



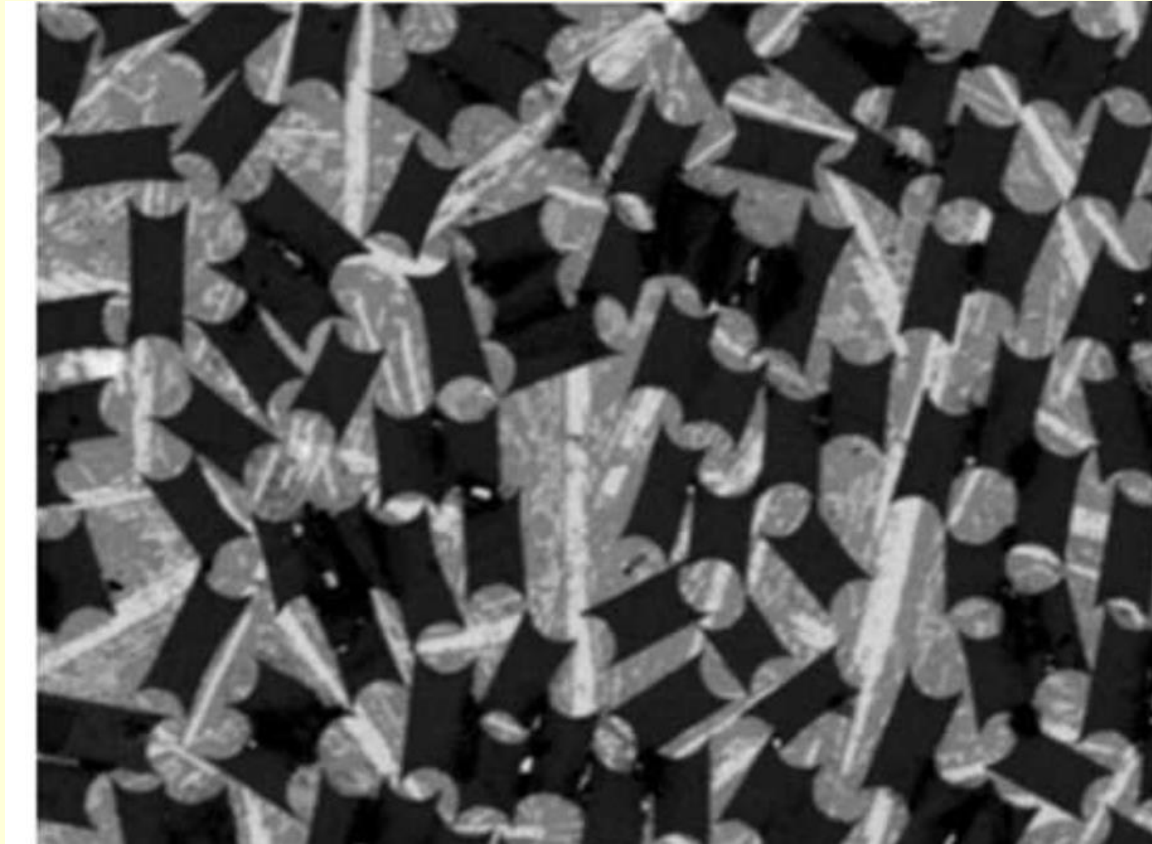
SEM MAG: 1.70 kx
HV: 20.0 kV
VanKV

DET: BSE Detector
DATE: 12/05/13
Device: Vega TS5130MM

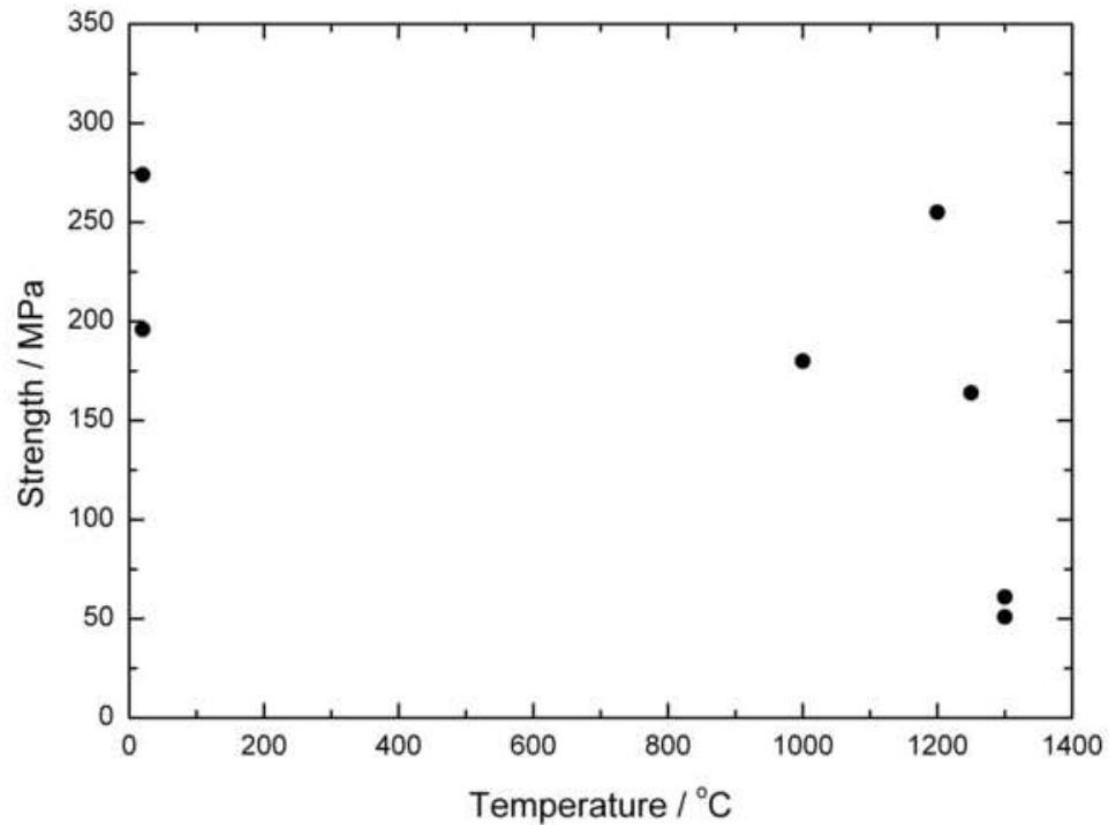


Vega ©Tescan
RSMA Group IEM RAS

Fibers $\text{Al}_2\text{O}_3\text{-Y}_3\text{Al}_5\text{O}_{12}\text{-ZrO}_2$ + matrix FeCoNiCrW



Strength temperature dependence of the composite with eutectic fiber $\text{Al}_2\text{O}_3\text{-Y}_3\text{Al}_5\text{O}_{12}\text{-ZrO}_2$ and FeCoNiCrW alloy matrix



***High-entropy superhard
coatings***

GB – engineering of nanostructured materials. “Theoretical” hardness

10 nm



$$H_v = E/10$$

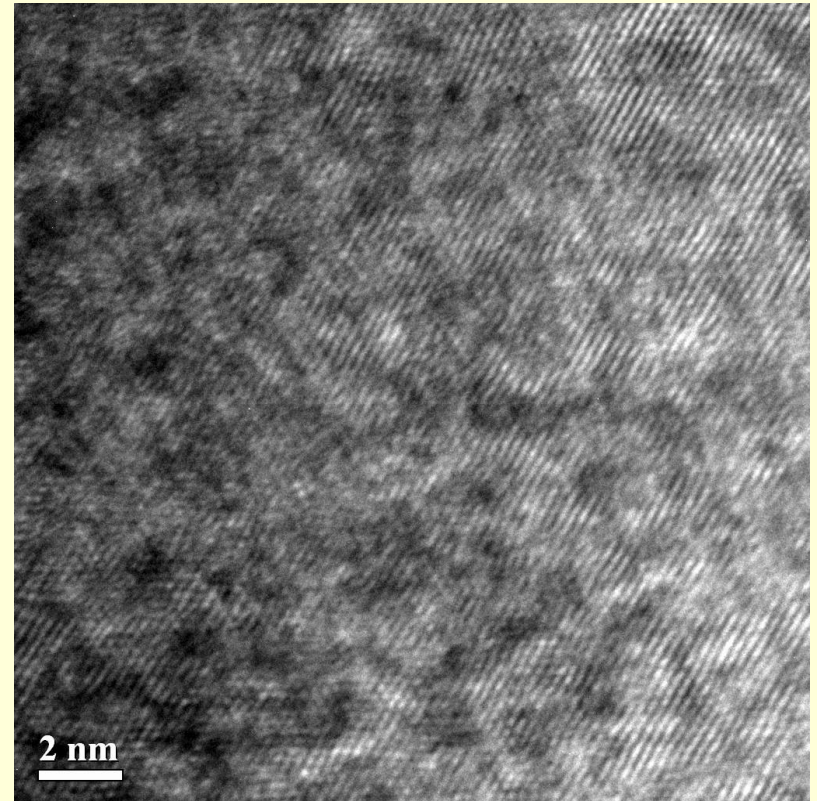
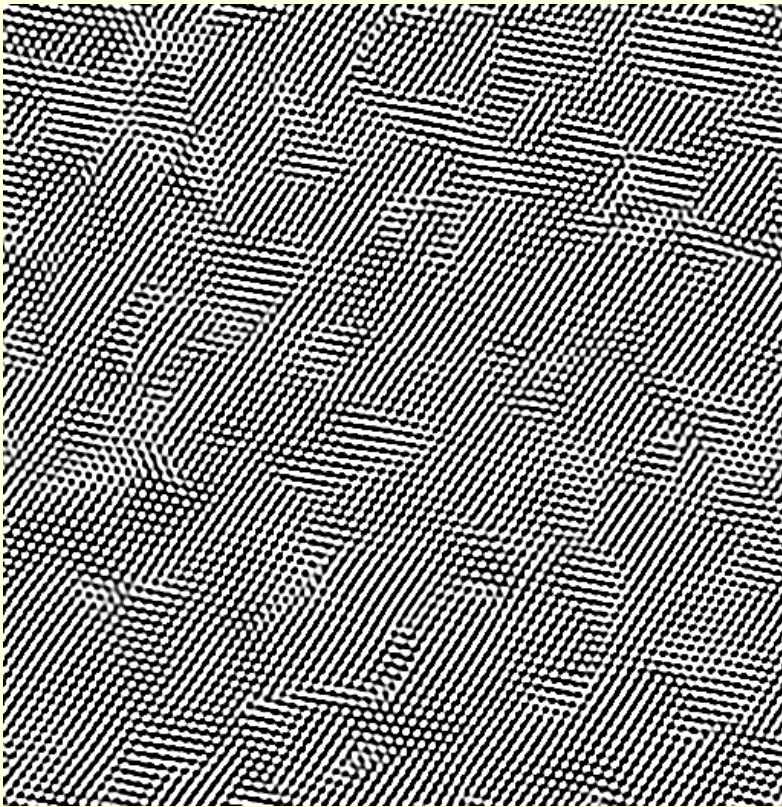
Properties of some high-entropy coatings

Coating compositions	Phase composition %, lattice parameter a, nm	H_{IT}, GPa	E_r, Gpa	H_{IT}/ E_r
TiVZrNbHfTa	BCC-100-0,3264	10,1±0.3	105±3	0,096
AlCrFeCoNiCuV	BCC-67,24-0, 2887 FCC-32,74- 0,3663	18.6±0.4	187±5	0,099
TiZrHfNbTaCr	c14 -75,36 -0,5164 BCC-24,64 -0,3284	19,0±0.6	192±8	0,099
Cr-Co-Cu-Fe-Ni,	FCC-0,3605	15,0	181	0.093
(TiVZrNbHfTa)N	FCC-0,4462	54,0 ±3	400 ±8	0,135

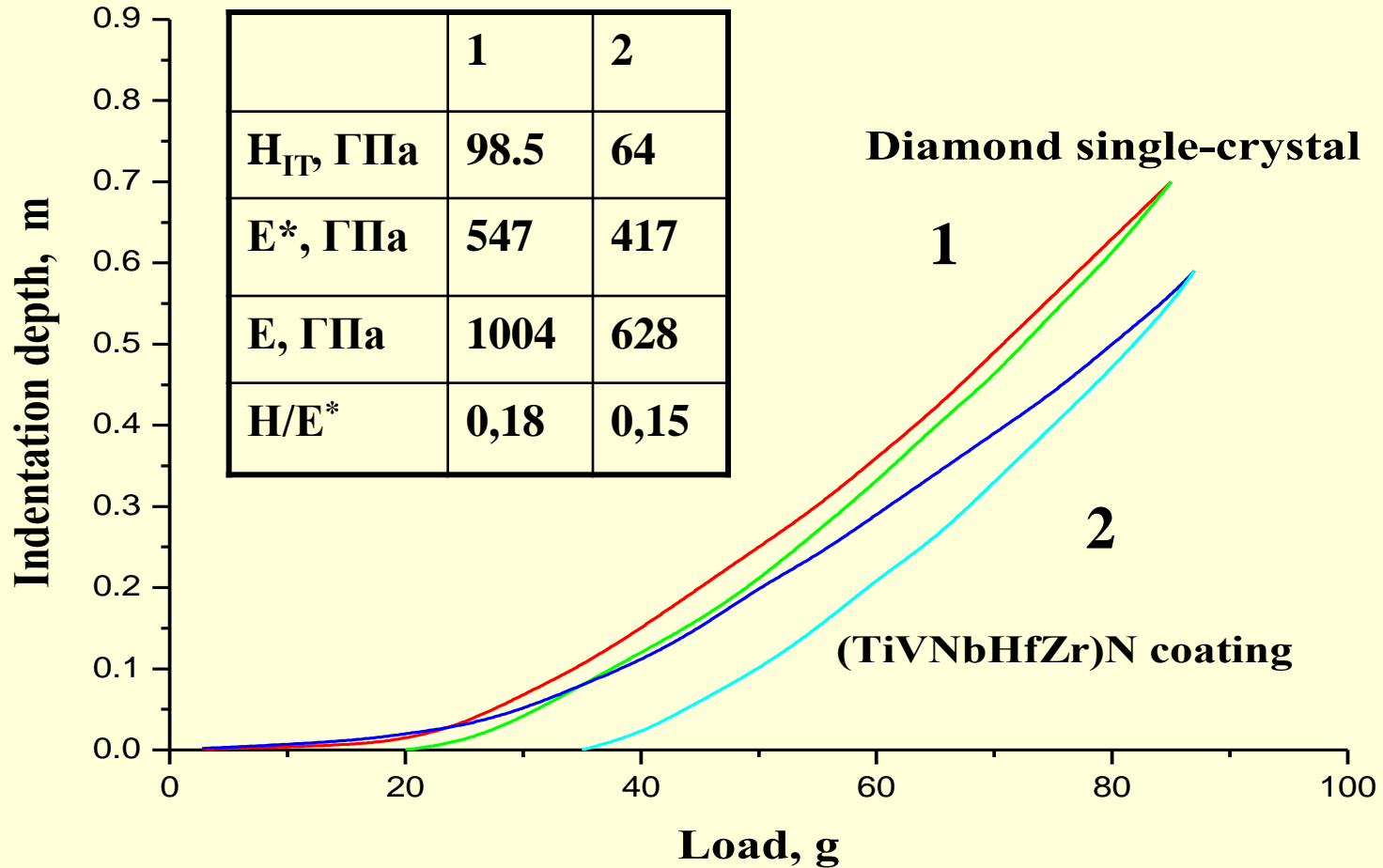
Properties of arc-coatings of 4 μm thickness based on Ti-V-Zr-Nb-Hf HEA

State	Structure	Lattice parameter, nm		H , GPa	E , GPa	H/E^*	E_{calc} , GPa
		Calcul.	Exper.				
As-cast	BCC	0,3350	0.3405	4.2	95	0,047	116
Coating in vacuum 10^{-4}	BCC	0.3350	0,3264	8,1	130	0,077	116
Coating at N_2 partial pressure $P_{\text{N}} = 0,66 \text{ Pa}$	FCC	0.4532	0,4462	64.0	620	0,138	460

Structure of Ti-V-Zr-Nb-Hf coating obtained by the arc deposition in vacuum (N_2 partial pressure of 0.66 Pa)

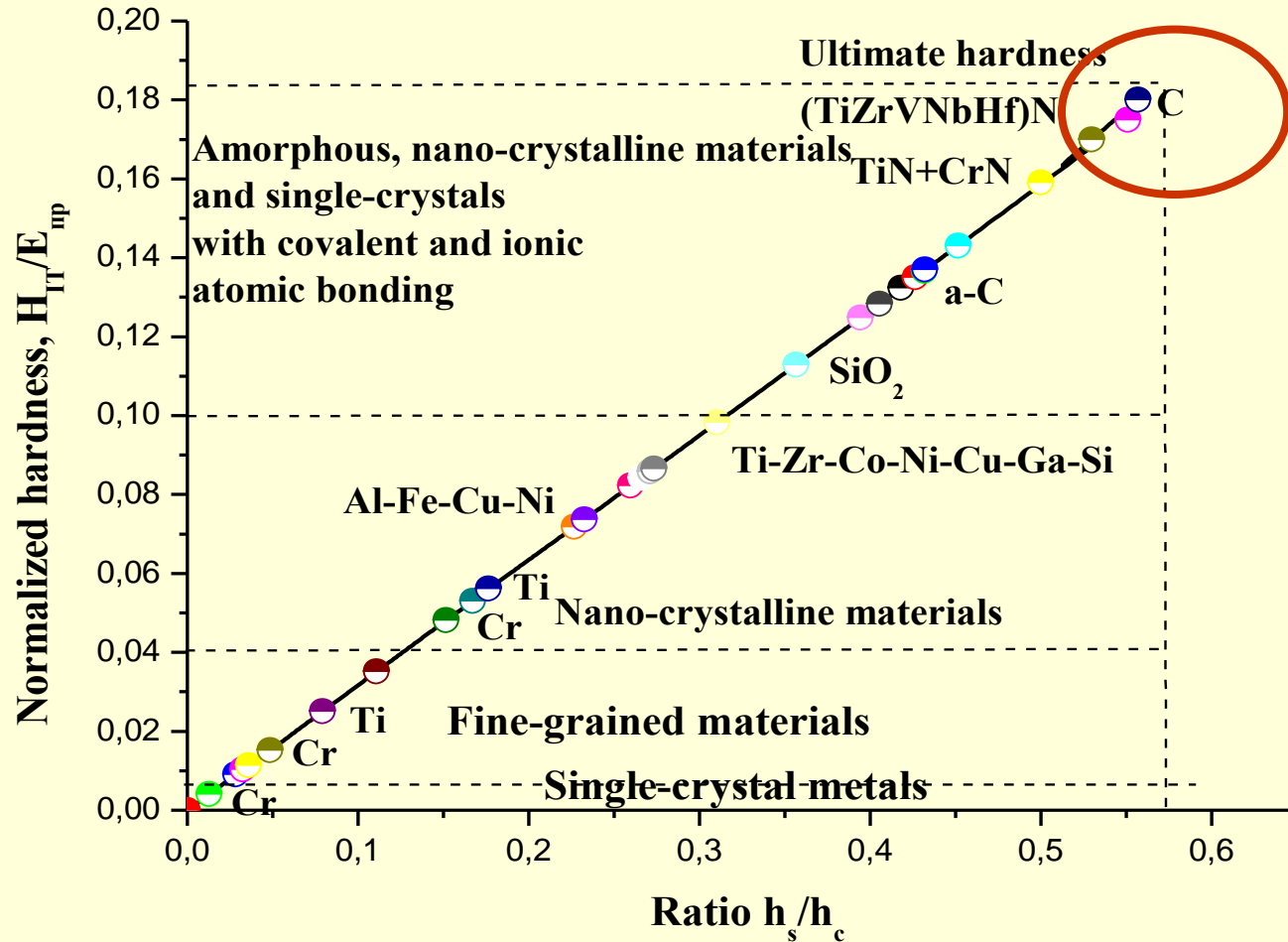


Comparative physical-mechanical properties of diamond and high entropy nitride coating obtained by indentation



Normalized Hardness of different materials

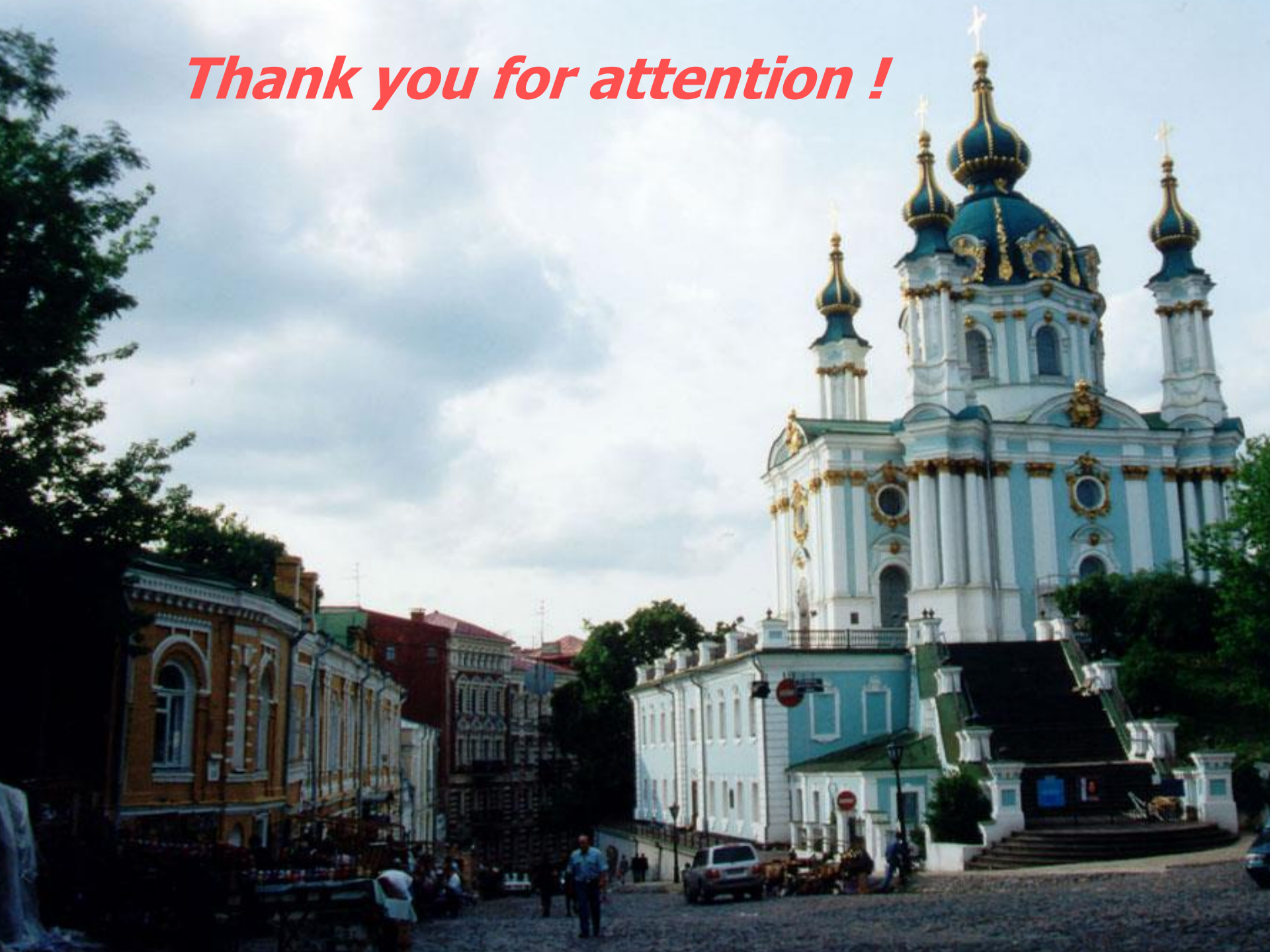
INDENTATION EQUATION $H / E^* = K \cdot (h_s / h_c)$



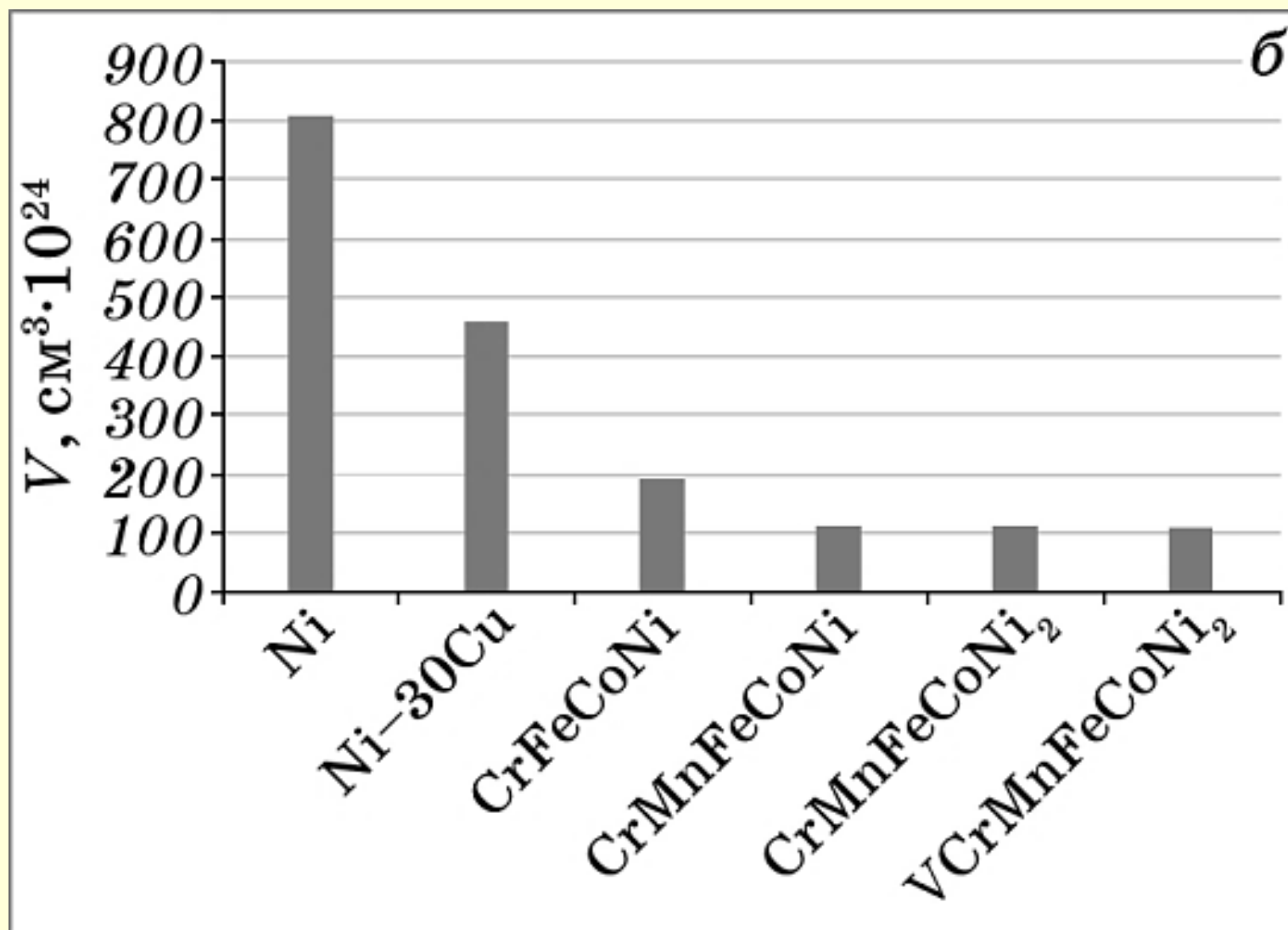
Conclusions

- **Non-obvious solid solution hardening is connected with:**
 - a) Pico-level lattice distortions.**
 - b) Nanoclusters in solid solution**
 - c) New features of GB-engineering in multi-component systems**
- **Temperature dependencies of yield stress demonstrate extended athermal plateau due to reasons listed above and may be due to sluggish diffusion and DSA**
- **New heat resistant multi-component (High-Entropy) alloys with a density of 3.8–4.0 and 7.4–7.8 g/cm³ can be created**
- **HEAs can be a good base for a new generation of heat resistant composites**
- **Prospective direction is a search of new radiation resistant multicomponent alloys consisted of low active elements**

Thank you for attention !



Activation volume



6

Activation energy for dislocations movement

